The Coexistence of the Poly(phospho-siloxo) Networks and Calcium Phosphates on the Compressive Strengths of the Acid-Based Geopolymers Obtained at Room Temperature

Hamed I. Riyap[1] · F. Kenne Tazune[1] · Daniel Fotio[3] · Hervé K. Tchakouté[1,2] · Charles P. Nanseu-Njiki[1] · Claus H. Rüscher[2]

Abstract

This work aims to investigate the coexistence of the poly(phospho-siloxo) networks and calcium phosphates on the compressive strengths of the acid-based geopolymers obtained at room temperature. Waste fired brick and phosphoric acid were used as an aluminosilicate and chemical reagent, respectively. Calcium aluminate hydrate was prepared by mixing calcium hydroxide from the calcined eggshell and calcined bauxite. Calcium silicate hydrate was obtained by the mixture of rice husk ash and calcium hydroxide. The molar ratios CaO/Al_2O_3 and CaO/SiO_2 in the calcium aluminate and calcium silicate hydrates are equals to 1.0. The X-ray patterns of the acid-based geopolymers indicate the broad hump structure between 18 and 38°(2θ). In addition to this broad band, those from the mixture of calcium sources show the reflection peaks of monetite and brushite. The compressive strength of the reference is 56.43 MPa. Those obtained with the addition of 10, 20, 40 and 50 g of calcined eggshell are 30.15, 22.85, 21.16 and 13.47 MPa, respectively. The ones from calcium aluminate hydrate are 32.62, 31.58, 17.83 and 16.33 MPa, respectively. Whereas those containing calcium silicate hydrate are 44.02, 42.71, 40.19 and 18.59 MPa, respectively. This work demonstrates that the formation of calcium phosphates in the structure of the acid-based geopolymers decreases the poly(phospho-siloxo) chains and therefore reduces their compressive strengths. The moderate addition of calcium silicate hydrate reduces slightly the compressive strengths of the acid-based geopolymers which can be comparable to the one of CEM II 42.5R.

Keywords Waste fired brick · Calcium sources · Acid-based geopolymers · Poly(phospho-siloxo) · Monetite · Brushite

1 Introduction

Geopolymer material is a class of semi-crystalline inorganic polymer with a three-dimensional structure constituted of poly(sialate-siloxo) or poly(phospho-siloxo) chains. This material is obtained from the chemical reactions between a semi-crystalline aluminosilicate source and alkaline reagents (sodium or potassium waterglass) or acid reagents (humic or phosphoric acids). Several researchers reported that the semi-crystalline aluminosilicates used for the preparation of this inorganic polymer could be natural raw materials such as kaolin [1] and volcanic ash [2–6], industrial by-products such as fly ash [7, 8] and ground granulated blast furnace slag [9] and synthetic material like metakaolin [10]. Among these raw materials, ground granulated blast furnace slag and fly ash denoted fly ash class C has approximately 40 and 20 wt% of calcium oxide, respectively [11]. Geopolymer networks obtained in an alkaline reagent from both latter raw materials indicated the coexistence of the calcium silicate hydrate (CSH) and/or calcium aluminate silicate hydrate (CASH) and the poly(sialate-siloxo) network in their structures. According to the findings work of Yip et al. [12], CSH and/or CASH present in the structure of the geopolymer material acts as filler or micro-aggregate and enhance its strength. Mabah et al. [13] and Tchakouté

✉ Hervé K. Tchakouté
htchak@yahoo.fr

[1] Laboratory of Analytical Chemistry, Department of Inorganic Chemistry, Faculty of Science, University of Yaounde I, P.O. Box 812, Yaounde, Cameroon

[2] Institut Für Mineralogie, Leibniz Universität Hannover, Callinstrasse 3, 30167 Hannover, Germany

[3] Department of Chemistry in Higher Teacher Training College, University of Maroua, P.O. Box 55, Maroua, Cameroon

et al. [14] used semi-crystalline CSH as an additive for the preparation of (Ca, Na)-geopolymer cements. These authors reported that the incorporation of 10 wt% of this calcium source enhances the compressive strength of the geopolymer cement. Mackenzie et al. [15] reported that the amorphous calcium silicate used as an additive includes in the geopolymer network and Tchuenté et al. [16] concluded that the compressive strengths of the specimens decrease with increasing the amorphous calcium silicate hydrate content in the geopolymer mortars. Yip et al. [11] used different crystalline calcium silicate sources such as Ordinary Portland cement, ground granulated blast furnace slag, wollastonite, hornblende, tremolite, prehnite and anorthite containing 64.70, 43.00, 47.50, 21.39, 22.57, 25.77 and 15.43 wt% of CaO, respectively, as additives to metakaolin for producing geopolymer cements. They reported that the substitution of metakaolin by 20 wt% of any calcium silicate source provides higher compressive strength value. Tchakouté et al. [17] used calcium phosphates such as brushite and hydroxyapatite as additives for producing geopolymer cements using sodium waterglass as chemical reagent. The reported that geopolymer cements containing 2 wt% of hydroxyapatite and 6 wt% of brushite provide higher compressive strengths. This indicates that the presence of calcium phosphate compounds in the structure of geopolymer cements from alkaline medium improve their compressive strengths. Gualtieri et al. [18] investigated the thermal properties of the acid-based geopolymer foams by in situ XRPD and Rietveld refinements using limestone as pore forming agent. They reported that β-Ca_3PO_4 is formed in the structure of the non-heated geopolymer. These authors did not say anything concerning the compressive strength. Apart geopolymer cement, other polymers such as poly(p-anisidine) nanocomposites have been prepared by Boutaleb et al. [19]. Up to now, no previous work does not investigate the behaviour of calcium phosphate compounds in the structure of acid-based geopolymers. Many researchers used metakaolin [20–22] and laterite [23, 24] as aluminosilicates for the production of the acid-based geopolymers. To obtain the hardened acid-based geopolymers, these authors cured the fresh paste at 60 °C in an oven for 24 h. According to Davidovits [25], geopolymer material obtained in an acidic medium requires an energy gradient which favours quickly the formation of the hardened material. In order to avoid the energy gradient during the synthesis of the acid-based geopolymers, it would be interesting to use an aluminosilicate source able to produce specimens which can be handled after maintained at room temperature of the laboratory and demoulded after 24 h.

This work deal to study the coexistence of the calcium phosphates and poly(phospho-siloxo) networks on the compressive strength of the acid-based geopolymers obtained at room temperature. Waste fired brick was used in this investigation as an aluminosilicate source. In order to avoid the energy gradient during the preparation of the acid-based geopolymer, Bewa et al. [26] showed that the obtained fresh paste of the acid-based geopolymer from waste fired brick hardened at room temperature of the laboratory and demoulded after 24 h. The coexistence of the calcium phosphate compounds and poly(phospho-siloxo) networks in the structure of the acid-based geopolymers were examined by measuring their compressive strengths. The X-ray diffractometry was performed in order to identify the calcium phosphates and the poly(phospho-siloxo) chains in the structure of the acid-based geopolymers. The functional groups and morphologies were monitored using the infrared spectroscopy and scanning electron microscopy, respectively.

2 Materials and Experimental Procedures

2.1 Materials

Waste fired brick provides by the Local Promotion Materials Authority (Mipromalo) was used as an aluminosilicate source in this investigation. This company is located in the Centre region of Cameroon. The chicken eggshells (calcium carbonate source) were harvested from nearby restaurant in Yaounde situated in the Centre region of Cameroon. This calcium-rich waste was washed with tap water and dried in air. Bauxite was collected in Minim-Martap in the Adamawa region of Cameroon. Rice husk ash denotes RHA with white colour was provided by the Upper Nun Valley Development Authority (UNVDA) situated in Ndop in the North-West region of Cameroon. One collected, waste fired brick and bauxite were broken using a hammer whereas dried chicken eggshells were broken with hand into smaller pieces. The fragments of waste fired brick, bauxite, pieces of chicken eggshells and rice hush ash were finely crushed separately for 30 min in the ball mill (MGS Srl) and sieved at 80 µm in order to get different smaller powders of each sample. The fine powders of waste fired brick, bauxite and chicken eggshells were denoted WB, BaX and Eggshell, respectively. The fine powders of eggshell and BaX were separately calcined in the electric programmable furnace (MGS Srl) at 900 and 600 °C, respectively for 2 h using a heating and cooling rate of 5 °C/min. The obtained calcined powders of eggshell and BaX were denoted Eggshell_900 and CBaX, respectively. Waste fired brick was already characterized by Bewa et al. [26]. They reported that this aluminosilicate-rich waste is constituted of around 61 wt% of silicon dioxide and has only approximately 8 wt% of quartz. Chicken eggshell and rice husk ash were characterized by Mabah et al. [13] and bauxite was characterized by Tchamba et al. [27]. The chemical compositions of these

Table 1 Chemical compositions of waste fired brick (WB), rice husk ash (RHA), eggshell, eggshell-900 and bauxite (BaX), wt%

Samples Oxides	WB	RHA	Eggshell	Eggshell-900	BaX
Na_2O	/	/	0.136	/	/
MgO	0.323	0.28	0.855	0.961	/
Al_2O_3	22.50	0.58	0.233	0.24	58.10
SiO_2	60.98	93.20	0.243	0.373	1.00
P_2O_5	0.331	/	0.476	0.491	0.17
SO_3	/	/	0.206	0.326	0.07
K_2O	0.932	3.05	0.071	/	/
CaO	0.104	0.57	/	96.355	0.08
$CaCO_3$	/	/	93.166	/	/
TiO_2	1.728	0.03	/	/	2.40
Cr_2O_3	0.0251	/	/	/	0.06
Fe_2O_3	9.635	2.20	0.085	0.11	5.54
ZnO	0.019	/	/	/	0.03
SrO	0.0049	/	0.288	/	0.05
ZrO_2	0.06185	/	/	/	0.08
Others	0.2008	1.78	/	/	0.75
LOI	3.10	1.2	/	/	31.67

LOI loss on ignition

raw materials are given in Table 1. The chemical reagent with molar concentration 10 M was prepared by a dilution of a commercial phosphoric acid with 85 wt% of purity and the specific gravity equal to 1.69. It was provided by Sigma Aldrich, France.

2.2 Experimental Procedures

2.2.1 Preparation of Semi-crystalline Calcium Aluminate Hydrate and Calcium Silicate Hydrate

In order to prepare the semi-crystalline calcium silicate hydrate and calcium aluminate hydrate, the powder of Eggshell_900 (CaO) was mixed mechanically with distilled water for around 5 min in the porcelain mortar to obtain gel of $Ca(OH)_2$. The prepared gel was separately mixed with rice hush ash and calcined bauxite for 30 min using a rapid ball mill in order to have the gel of semi-crystalline calcium silicate hydrate and calcium aluminate hydrate with molar ratios CaO/SiO_2 and CaO/Al_2O_3 equal to 1.0. These homogeneous and $Ca(OH)_2$ gels were dried in an electric oven (GenLabPrime) at 80 °C for 24 h. The different agglomerated specimens obtained were separately crushed in a rapid ball mill for 30 min to get the powders of semi-crystalline calcium silicate hydrate and calcium aluminate hydrate named CS et CA, respectively. Calcined eggshell, semi-crystalline calcium silicate and calcium aluminate hydrates were used in this work as calcium sources.

2.2.2 Synthesis of acid-Based Geopolymer Cements Containing Calcium Phosphates

Acid-based geopolymer cements without or containing calcium phosphates were prepared by mixing separately phosphoric acid solution to the powders of waste fired brick, the mixture of waste fired brick and calcined eggshell or semi-crystalline calcium silicate hydrate or semi-crystalline calcium aluminate hydrate. It is worth to mention that the mixture of waste fired brick and Eggshell_900, waste fired brick and CS, waste fired brick and CA were obtained by the addition of 10, 20, 40 and 50 g of Eggshell_900 or CS or CA to 100 g of waste fired brick. Each whole mixture of the material was blended mechanically in a porcelain mortar for about 5 min and each fresh paste was moulded in the cubic moulds with the dimension of $40 \times 40 \times 40$ mm. The moulded samples were cured at room temperature for 24 h, demoulded and sealed in the plastic bag for 28 days at 25 ± 2 °C with 68% of humidity. The acid-based geopolymer from the powders of waste fired brick and phosphoric acid was denoted GPWBA (called reference). Those obtained from the addition of 10, 20, 40 and 50 g of Eggshell_900 to 100 g of waste fired brick were labelled GWBEg10, GWBEg20, GWBEg40 and GWBEg50, respectively. Those from 100 g of waste fired brick and 10, 20, 40 and 50 g of CS were called GWBCS10, GWBCS20, GWBCS40 and GWBCS50, respectively. The ones from 100 g of waste fired brick and 10, 20, 40 and 50 g of CA were called GWBCA10, GWBCA20, GWBCA40 and GWBCA50, respectively.

2.3 Methods of Characterisation of Starting Materials and Acid-Based Geopolymer Cements

The coexistence of calcium phosphates and poly(phosphosiloxo) networks were studied by the determination of the compressive strengths, mineralogical compositions and the functional groups in the structures of the acid-based geopolymers. The compressive strengths of each specimen were measured according to PR EN/ISO 679 standard using an automatic hydraulic press (Impact Test Equipment Limited, UK KA20 3LR) with a 250 kN capacity. They were measured on the cubic moulds maintained for 28 days at room temperature of the laboratory. The compressive strengths were determined using a loading rate kept constant at 0.50 MPa/s. All tests were done on the three parallel specimens and the arithmetic mean value was adopted as the final value of the compressive strength and standard deviation of each composition. After measuring the compressive strength, the fragments of the selected samples were used to observe the

morphology of the final products. Others samples were finely pulverized in the ball mill and used to determine the mineralogical compositions and functional groups present in the structure of the obtained specimens.

The mineralogical compositions of bauxite, calcined bauxite, semi-crystalline calcium aluminate hydrate, semi-crystalline calcium silicate hydrate and the selected acid-based geopolymers were performed on a X-ray diffractometer named Bruker D4. The X-ray pattern of each specimen was recorded using CuKα radiation at 40 kV and 40 mA between 5 and 80° (2θ) for 7 h in steps of 0.03°. The crystalline phases present in the structure of each sample were identified using X'Pert HighScore Plus software.

The functional groups were evaluated using KBr method on an infrared spectrometer denoted Bruker Vertex 80v. The infrared spectrum of each sample was registered with a resolution of 2 cm^{-1} and 32 scans using the pellet prepared by the addition of about 200 mg of KBr to around 1 mg of BaX or CBaX or CS or CA or the selected acid-based geopolymers.

The micrography images with ×100 and ×1000 magnifications of the fragments of the reference acid-based geopolymer and those containing 10, 20 and 40 g of each calcium source after gold-coating were observed using a JEOL JSM-6390A Scanning Electron with an acceleration voltage of 30.0 kV.

3 Results and Discussion

3.1 Characterization of Raw Materials and Calcium Sources

The X-ray patterns and infrared spectra of chicken eggshell and calcined eggshell are presented in Figs. 1 and 2, respectively. They are already discussed by Mabah et al. [13].

3.1.1 X-ray Patterns

The X-ray patterns of waste fired brick (WB) and rice husk ash (RHA) are displayed in Fig. 3. Those of bauxite and calcined bauxite are depicted in Figs. 4 and 5 illustrate the X-ray patterns of semi-crystalline calcium silicate hydrate (CS) semi-crystalline calcium aluminate hydrate (CA) and calcium hydroxide. The X-ray patterns of waste fired brick and rice husk ash indicate the halo diffractions between 15 and 35°(2θ) and ranging from 15 to 45°(2θ), respectively. These halo diffractions correspond to the presence of amorphous aluminosilicate phase and amorphous silica in the structure of waste fired brick and rice husk ash, respectively. In addition to these amorphous phases, the one of waste fired brick shows the reflection peaks of illite, quartz, anatase, hematite (broad peaks) and the residual peak of kaolinite. Whereas the one of rice husk ash indicates the reflection peaks of cristobalite. The X-ray patterns of bauxite (BaX) and calcined bauxite (CBaX) depicts in Fig. 4 present the peaks of gibbsite only on the X-ray pattern of BaX, kaolinite,

Fig. 1 X-ray patterns of eggshell and calcined eggshell (Eggshell_900). C and CaO denote the reflection peaks of calcite and calcium oxide, respectively
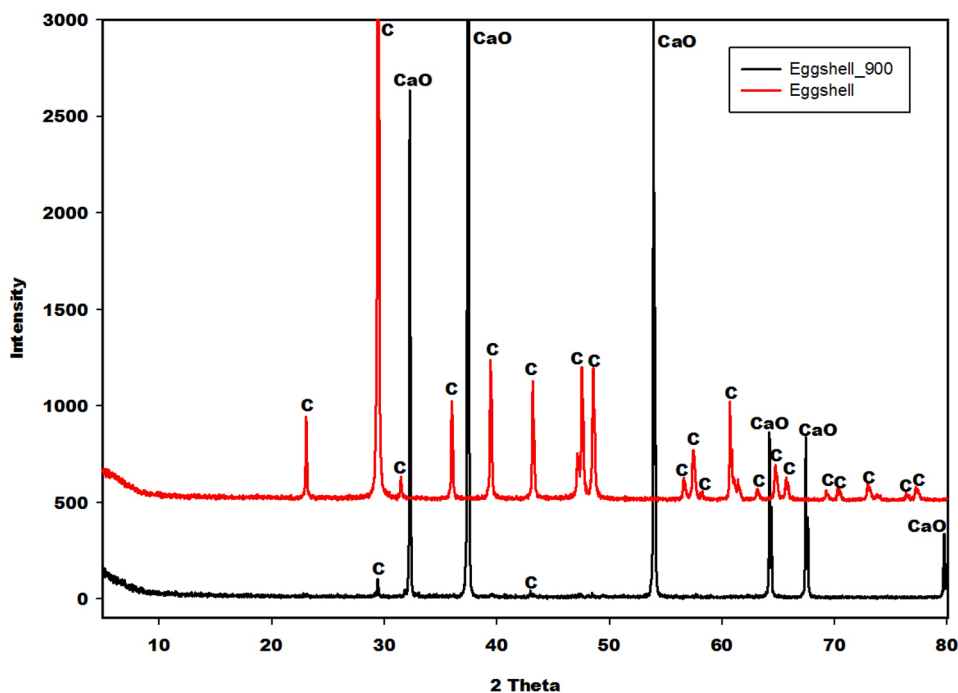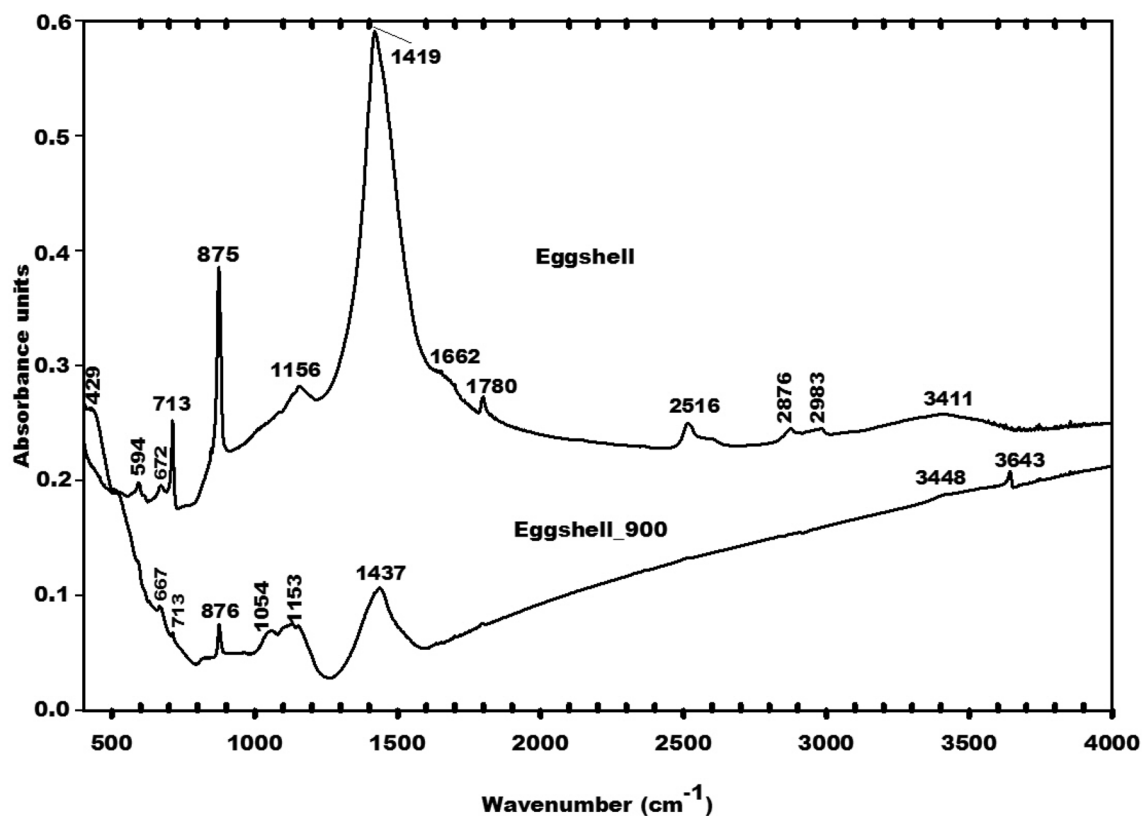
Fig. 2 Infrared spectra of eggshell and calcined eggshell (Eggshell_900)

hematite, anatase and the lower reflection peaks of quartz. In addition to these crystalline phases, the diffractogram of calcined bauxite shows a slightly broad hump structure in the range 18–53°(2θ) belongings to the amorphous alumina and the trace of metakaolinite. It also indicates the broad peak at around 67°(2θ) corresponding to the amorphous alumina. The X-ray patterns of the semi-crystalline calcium silicate hydrate and semi-crystalline calcium aluminate hydrate reported in Fig. 5 indicate the reflection peaks of calcium hydroxide which are compared to the pattern of the portlandite [Ca(OH)$_2$] obtained by adding distilled water to the calcined eggshell (CaO). The X-ray pattern of semi-crystalline calcium silicate hydrate reported also the peaks of cristobalite and the broad band situated between 18 and 45°(2θ). This broad band corresponds to the amorphous phase contained in the structure of the semi-crystalline calcium silicate hydrate. In addition to the reflection peaks of calcium hydroxide, the X-ray pattern of the semi-crystalline calcium aluminate hydrate indicates the peaks of calcium aluminum oxide carbonate hydrate (CaAOC) and calcium aluminum oxide hydrate (CAOH) associated with quartz, anatase and hematite. The formation of CaAOC could be ascribed to the carbonation of CA. The amorphous alumina is observed at around 35.96, 42.63, 55.26 and 67.47°(2θ) and the broad amorphous phase between 20 and 52°(2θ).

3.1.2 Infrared Spectra

The infrared spectra of waste fired brick and rice hush ash illustrate in Fig. 6 indicate the absorption bands at 470 and 792–799 cm^{-1} corresponding to the bending and stretching vibration modes, respectively, of the siloxane (Si–O-Si) bonds of amorphous silica. The bands at 620 and 1199 cm^{-1} on the infrared spectrum of rice husk ash are ascribed to the bending and stretching vibration modes, respectively of Si–O–Si bonds of α-cristobalite [28]. The one at 1098 cm^{-1} is ascribed to the stretching vibration modes of amorphous silica. The absorption band at 1640–1643 cm^{-1} observed on both spectrums is ascribed to the stretching vibrations of H–O–H of water molecules. The one at 538 cm^{-1} on the infrared spectrum of WB is ascribed to the bending vibration modes of Si–O–Al with Al in VI-fold coordination. The absorption bands at 696 and 780 cm^{-1} observed on the infrared spectrum of WB is attributed to the stretching vibrations of Si–O–Si of quartz [29]. Those with low intensities at 915, 3626 and 3701 cm^{-1} on the spectrum of waste fired brick are ascribed to the stretching vibration modes of Al^{VI}–O corresponding to the residual kaolinite. The presence of the trace of kaolinite is confirmed by the appearance of the main reflection peak of kaolinite at around 12.22°(2θ) on
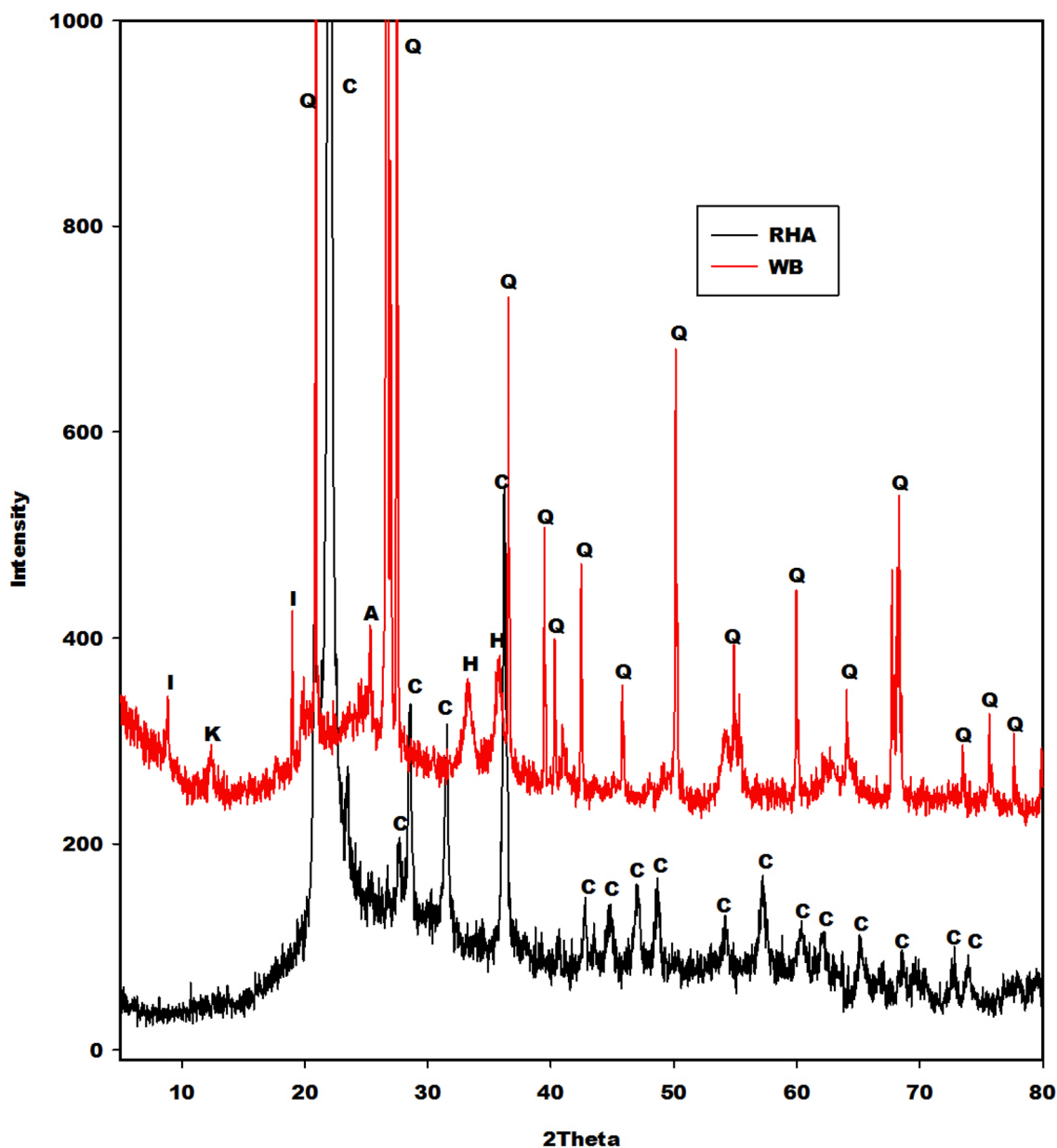
Fig. 3 X-ray patterns of rice husk ash (RHA) and waste fired brick (WB). C, I, K, A, Q and H denote the reflection peaks of cristobalite, illite, kaolinite, anatase, quartz and hematite, respectively

the XRD pattern of WB. The wavenumber of the main band of WB that appears at 1064 cm^{-1} is ascribed to the asymmetrical and symmetrical stretching vibration modes of Si–O–Si and Si–O–Al bonds. The infrared spectra of bauxite (BaX) and calcined bauxite (CBaX) are shown in Fig. 7. The spectrum of BaX shows four absorption bands at 3623, 3529, 3461 and 3382 cm^{-1}. According to Frost et al. [30], these bands are assigned to the stretching vibrations of hydroxyl groups (O–H) of gibbsite. The absorption bands at 3699 and 3623 cm^{-1} on the infrared spectra of BaX and CBaX are attributed to the stretching

vibration modes of hydroxyl groups (O–H) of kaolinite. The presence of the kaolinite on the spectra of both samples and gibbsite on the spectrum of bauxite is consistent with the X-ray patterns reported in Fig. 4. The infrared spectra of BaX and CBaX indicate the absorption band with the lowest intensity at about 1635 cm^{-1} corresponding to the bending vibration modes of water molecules in the structure of both samples. It can be observed that the absorption bands (3382, 3461 and 3529 cm^{-1}) which are previously attributed to the gibbsite on the infrared
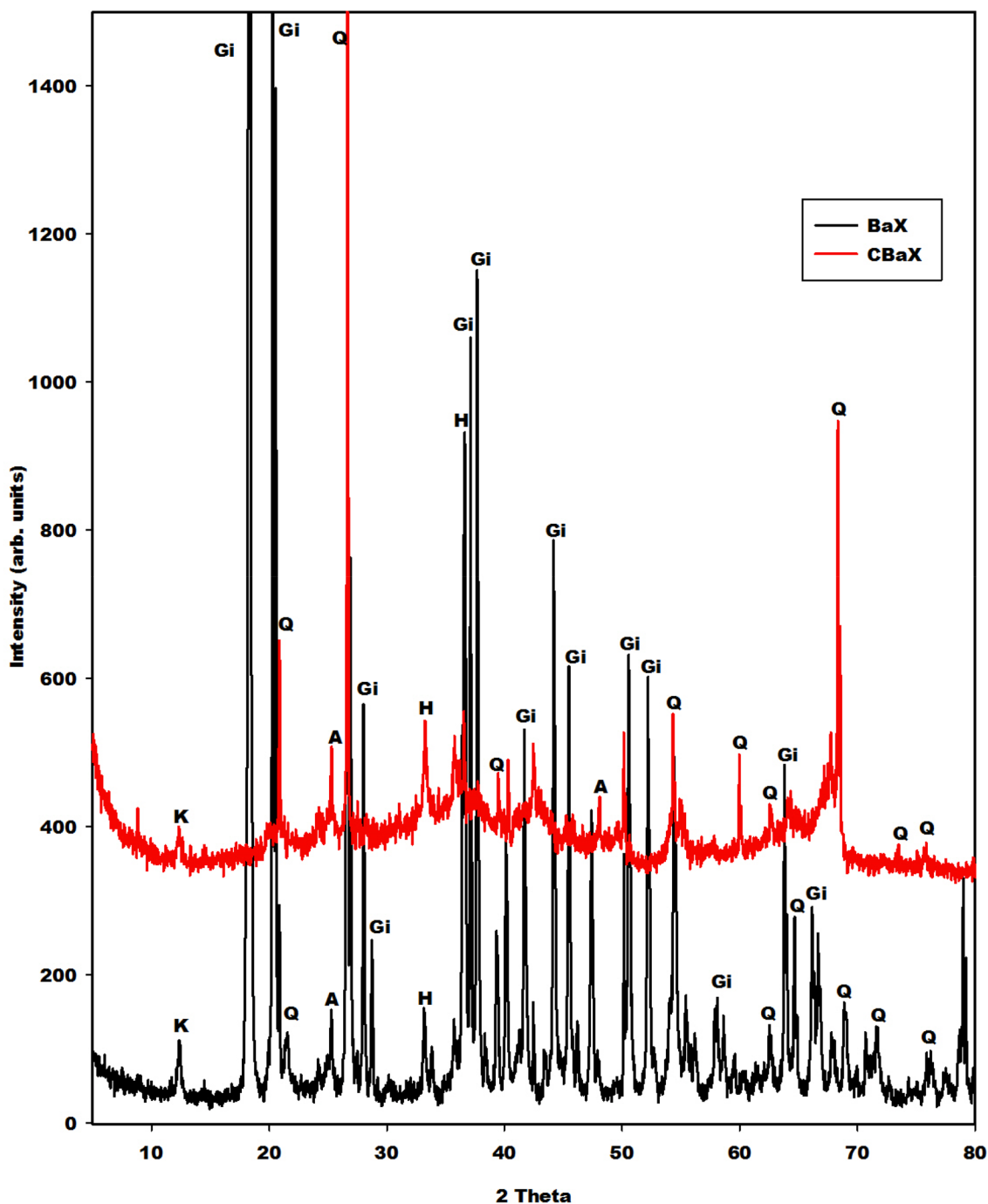
Fig. 4 X-ray patterns of bauxite (BaX) and calcined bauxite (CBaX). K, Gi, Q, A and H denote the reflection peaks of kaolinite, gibbsite, quartz, anatase and hematite, respectively

spectrum of bauxite (BaX) disappear on the spectrum of calcined bauxite (CBaX). This leads to the formation of a broad band at around $3491 \ cm^{-1}$. The disappearance of these three bands is ascribed to the transformation of gibbsite to amorphous alumina following Eqs. (1) and (2). This is also confirmed on the X-ray diffractogram of CBaX

by the disappearance of the reflection peaks of gibbsite (Fig. 4).

$$Al(OH)_3 \xrightarrow{290 \ °C} AlOOH + H_2O\uparrow$$
Gibbsite   Boehmite

(1)
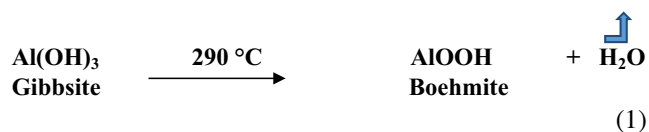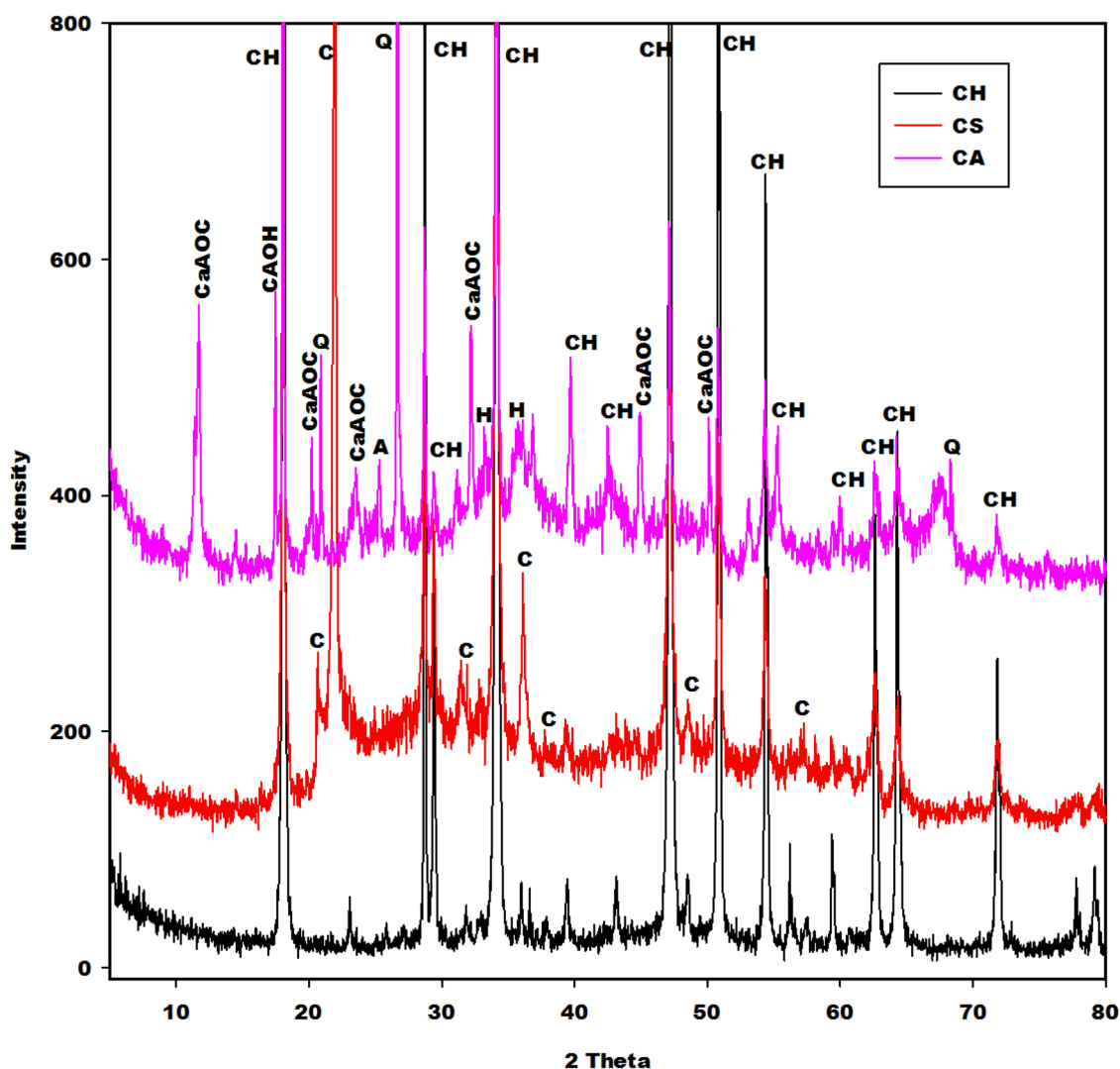
Fig. 5 X-ray patterns of portlandite (CH), semi-crystalline calcium silicate hydrate (CS) and semi-crystalline calcium aluminum hydrate (CA). CH, C, CaAOC, CAOH, Q, A and H denote the reflection peaks of calcium hydroxide, cristobalite, calcium aluminum oxide carbonate hydrate, calcium aluminum oxide hydrate, quartz, anatase and hematite, respectively

$$2\text{AlOOH} \xrightarrow{\text{475-550 °C}} \text{Al}_2\text{O}_3 + \text{H}_2\text{O}$$
Boehmite → Amorphous alumina

(2)
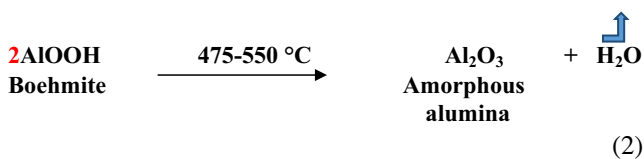
According to Frost et al. [29, 31], the absorption bands at 1021, 968 and 912 cm^{-1} on the spectrum of BaX are attributed to the deformation vibration modes of O–H. The bands at 803, 750, 663, 558 and 516 cm^{-1} are attributed to the stretching and bending vibrations of AlO_6 [32]. Pan et al. [33] reported that the absorption band at 471 cm^{-1} observed on the infrared spectrum of calcined bauxite is recorded to the stretching vibrations of sialate (Al–O–Si) bonds. The one at 543 cm^{-1} on the infrared spectrum of

CBaX records to the bending vibration modes of Al-O bonds in the octahedral AlO_6. The absorption bands at 795 and 1040 cm^{-1} on the spectrum of CBaX are assigned to the stretching vibrations of Al-O in the AlO_4 tetrahedra and Al–OH bonds, respectively [34]. Calcium hydroxide (CH) prepared by mixing Eggshell_900 (CaO) and distilled water and semi-crystalline calcium silicate hydrate (CS) present in Fig. 8 are already described by Tchakouté et al. [14]. The infrared spectrum of the semi-crystalline calcium aluminate hydrate (CA) reported in Fig. 8 indicates the absorption bands at 874 and 1420 cm^{-1}. They are ascribed to the vibration modes of C–O of carbonate ions (CO_3^{2-}) in the structure of the prepared semi-crystalline calcium aluminate hydrate. This is consistent with the apparition of the reflection peaks of calcium aluminum
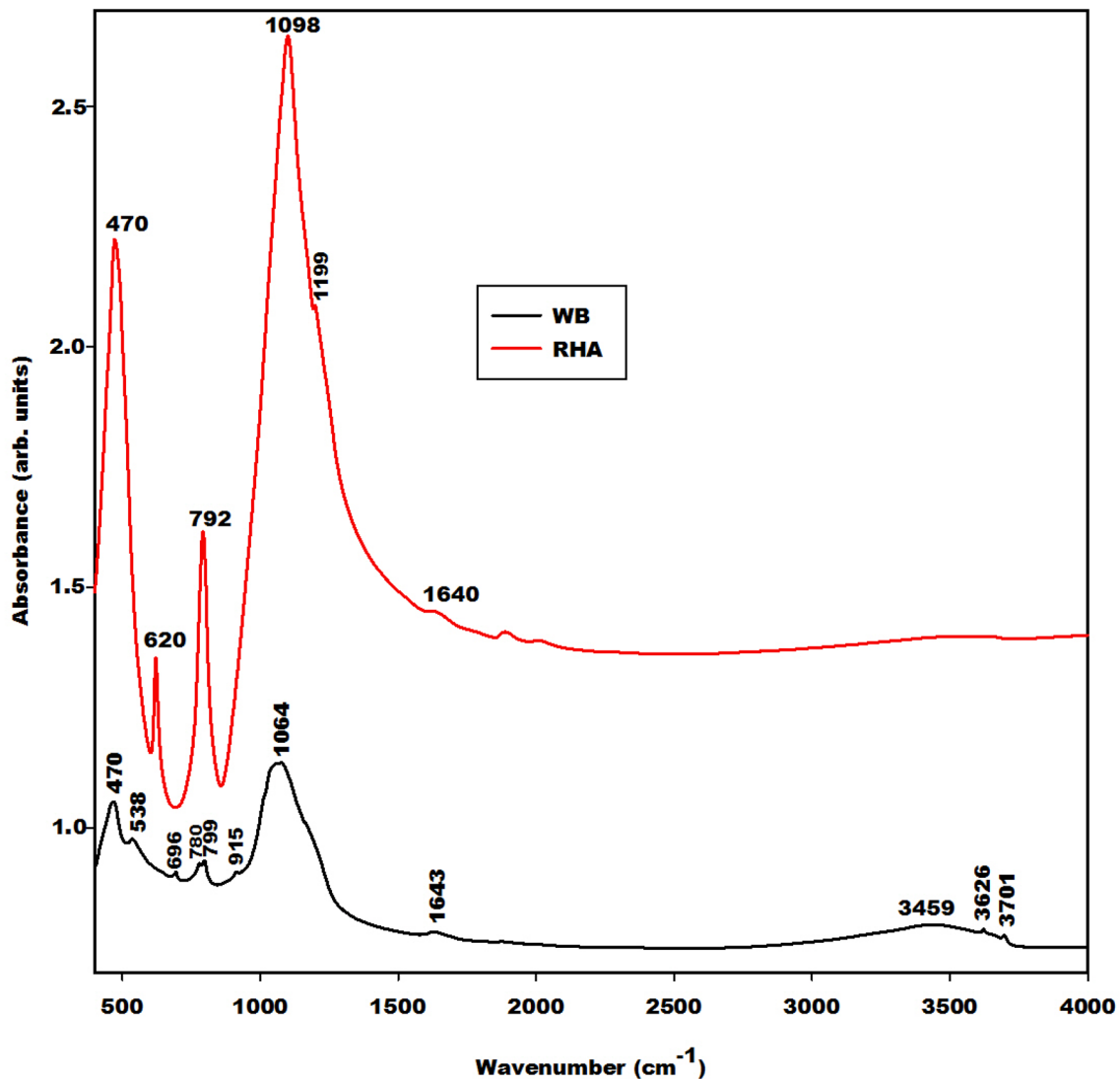
Fig. 6 Infrared spectrums of rice husk ash (RHA) and waste fired brick (WB)

oxide carbonate hydrate observed on the X-ray pattern of CA. The band at 539 cm^{-1} is assigned to the bending vibrations of Al-O bonds in the AlO$_6$ octahedral. The one at 916 cm^{-1} is recorded to the vibration modes of aluminol groups (Al–OH) in the structure of the semi-crystalline calcium aluminate hydrate. The presence of the bands at 1642 and 3472 cm^{-1} confirms the formation of water molecules and aluminol groups. According to Zidi et al. [34], the bands at 1040 and 1104 cm^{-1} on the spectrum of the semi-crystalline calcium aluminate hydrate are ascribed to the vibration modes of Al–OH bonds. Baltakys et al. [35] reported that the absorption band with higher intensity at 3642 cm^{-1} on the infrared spectrum of the prepared semi-crystalline calcium aluminate hydrate and calcium silicate hydrate is assigned to the vibration modes of O–H of calcium hydroxide or portlandite.

3.2 Characterization of Acid-Based Geopolymer Cements

3.2.1 X-ray Patterns

Figure 9 illustrates the X-ray patterns of the acid-based geopolymer cements prepared by adding 0, 10, 20 and 40 g of the calcined eggshell (Eggshell_900) or calcium silicate hydrate (CS) or calcium aluminate hydrate (CA) separately to 100 g of waste fired brick powders. The X-ray patterns of all specimens present the reflection peaks of illite, anatase, quartz, hematite and the trace of kaolinite. These minerals are also observed on the diffractogram of waste fired brick (Fig. 3). In addition to these phases, the X-ray patterns of the specimens obtained by adding 10, 20 and 40 g of Eggshell_900 (CaO) or CA indicate the peaks of monetite (CaHPO$_4$) and brushite (CaHPO$_4$.

Fig. 7 Infrared spectrums of bauxite (BaX) and calcined bauxite (CBaX)

$2H_2O$). The formation of monetite and brushite on the X-ray patterns of the acid-based geopolymers from the addition of Eggshell_900 to waste fired brick is obtained according to Eq. (3). In addition to monetite, the ones obtained when CA was added to the waste fired brick show the reflection peaks of augelite $[Al_2(PO_4). (OH)_3]$ which is ascribed to the dealumination of the semi-crystalline calcium aluminate hydrate in a phosphoric acid solution (Eq. 4). The presence of monetite on the X-ray patterns of the acid-based geopolymer cements when CS was added to the waste fired brick powders is justified by Eq. (5). And the presence of the additional silanol groups could be assigned to the dissolution of the amorphous silica from rice husk ash during the depolymerisation of the raw materials (a mixture of waste fired brick and calcium silicate hydrate).

$$Eggshell\_900 (CaO) + 2H_3PO_4 \longrightarrow CaHPO_4 + CaHPO_4. 2H_2O$$
$$\text{Monetite} \qquad \text{Brushite}$$
(3)

$$CA (CaO, Al_2O_3, H_2O) + 2H_3PO_4 \longrightarrow CaHPO_4 + [Al_2(PO_4). (OH)_3]$$
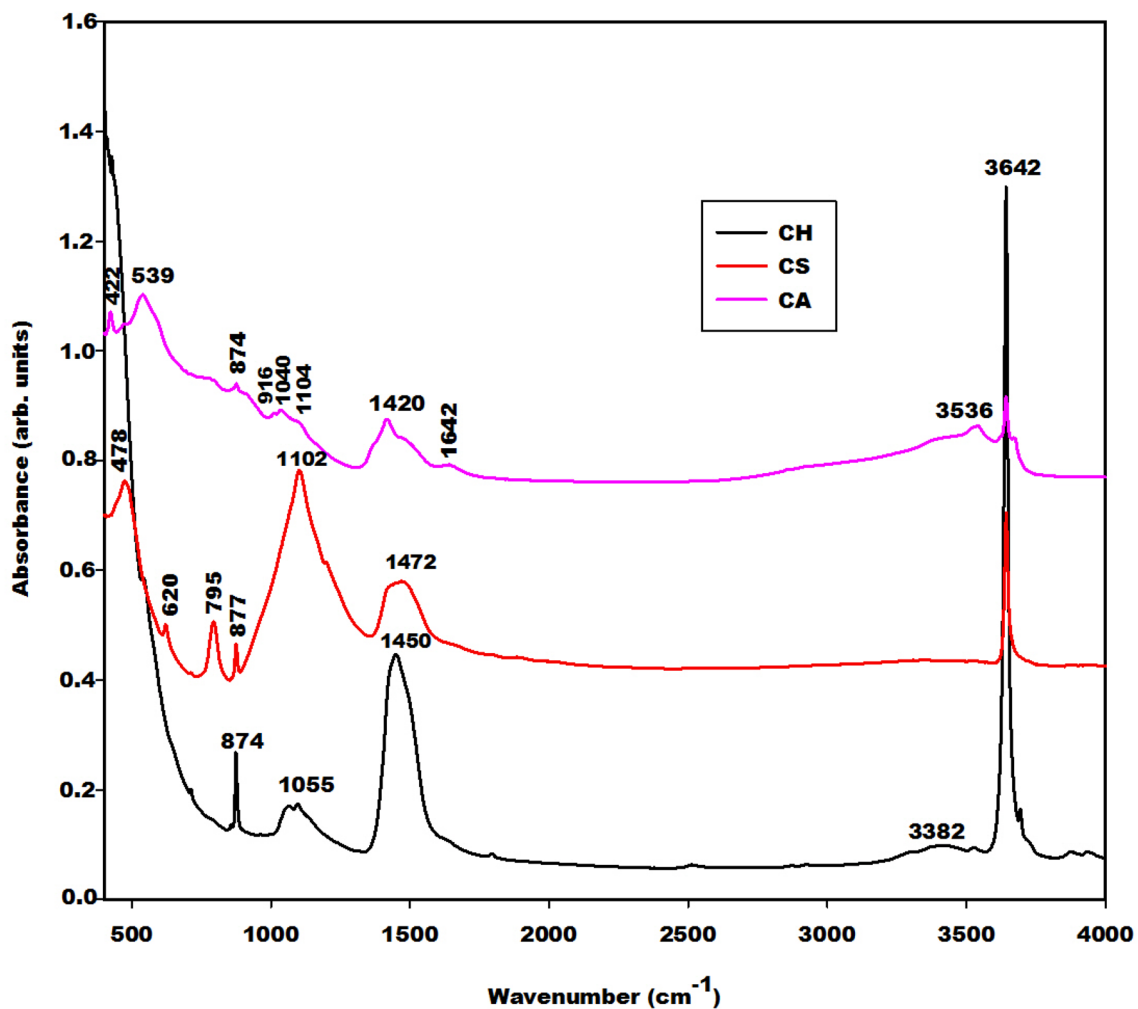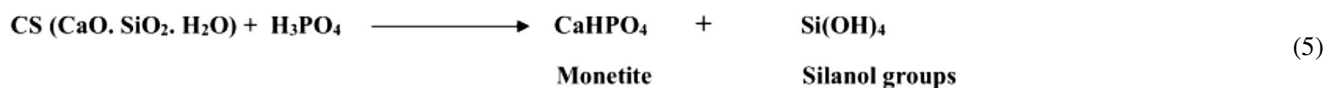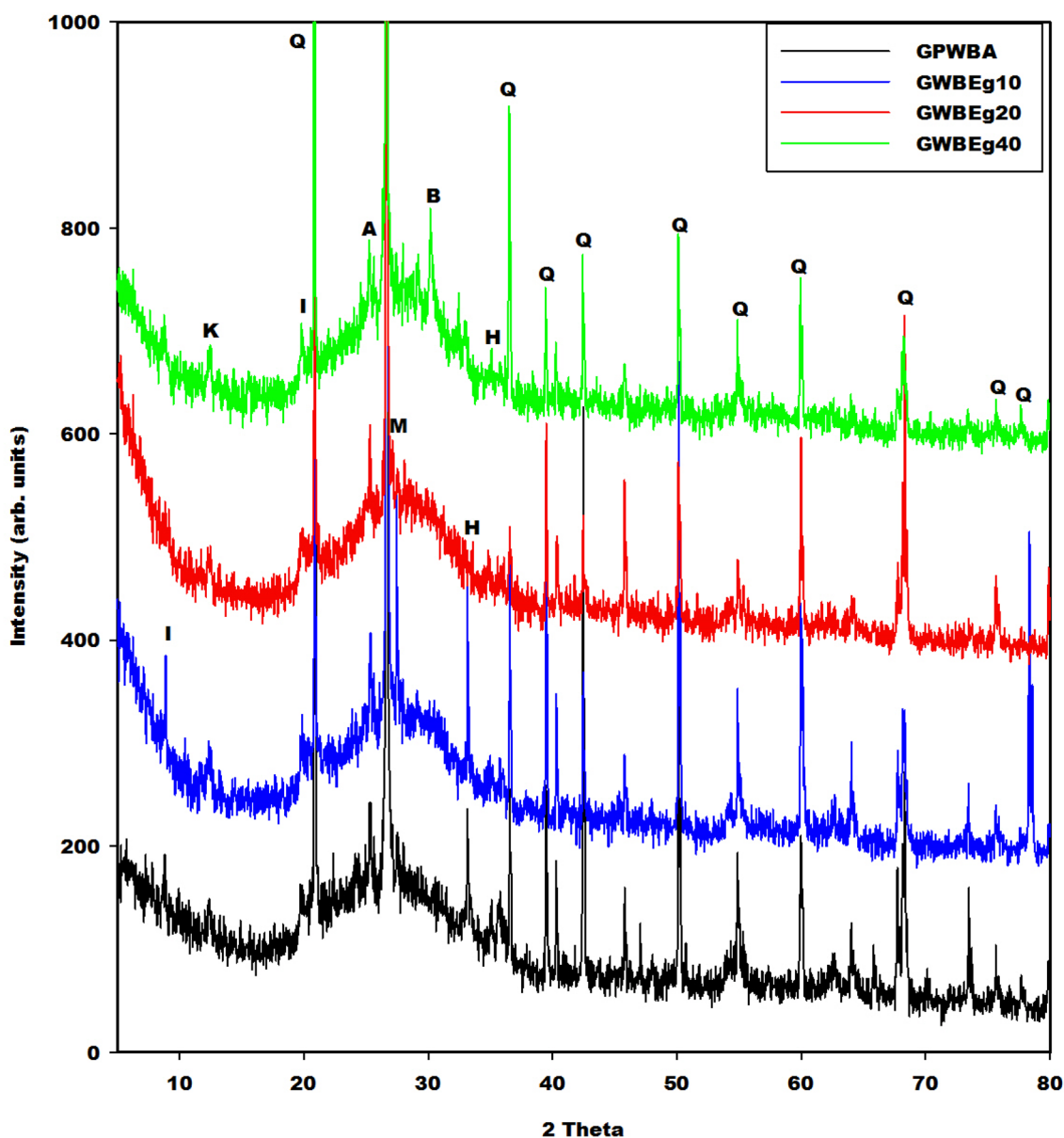$$\text{Monetite} \qquad \text{Augelite}$$
(4)

Fig. 8 Infrared spectra portlandite (CH), semi-crystalline calcium silicate hydrate (CS) and semi-crystalline calcium aluminate hydrate (CA)

$$CS\ (CaO.\ SiO_2.\ H_2O) + H_3PO_4 \longrightarrow \underset{\text{Monetite}}{CaHPO_4} \quad + \quad \underset{\text{Silanol groups}}{Si(OH)_4} \tag{5}$$

It is worth to note that these calcium phosphate compounds have clearly appeared on the X-ray patterns of the specimens when 40 g of each calcium source was added to waste fired brick powders. The X-ray patterns of the specimens from the mixture of waste fired brick powders and the semi-crystalline calcium silicate hydrate indicate the main reflection peaks of cristobalite. This mineral is observed on the X-ray pattern of rice husk ash (Fig. 3) used for its preparation (Fig. 5). Beside these crystalline minerals, the X-ray patterns of the different acid-based geopolymer cements show the broad hump structure ranging from 18 to 38°(2θ). This band appears in the range 15–32°(2θ) on the X-ray pattern of waste fired brick (Fig. 3). This suggests the formation of the poly(phospho-siloxo) network (amorphous phase) in the structure of the phosphate-based geopolymer cements. The presence of the poly(phospho-siloxo) network and calcium phosphates (brushite, monetite) and augelite imply the coexistence of these compounds in the structures of the prepared phosphate-based geopolymers. This indicates that during the synthesis of the acid-based geopolymers, one part of phosphoric acid reacts with the metakaolinite contained in the structure of waste fired brick and others react with calcium from different calcium sources added.

Fig. 9 X-ray patterns of the acid-based geopolymers. K, I, H, A, Q, C, B, M and Au denote the reflection peaks of the trace of kaolinite, illite, hematite, anatase, quartz, cristobalite, brushite, monetite and augelite, respectively

3.2.2 Infrared Spectra

The infrared spectra of the acid-based geopolymer cements prepared by adding 0, 10, 20 and 40 g of the calcined eggshell (Eggshell_900): GPWBA, GWBEg10, GWBEg20 and GWBEg20 or semi-crystalline calcium silicate hydrate (CS): GPWBA, GWBCS10, GWBCS20 and GWBCS20 or semi-crystalline calcium aluminate hydrate (CA): GPWBA, GWBCA10, GWBCA20 and GWBCA20 separately to 100 g of waste fired brick powders are depicted in Fig. 10. The spectra of all acid-based geopolymer cements indicate nearly the same absorption bands except

those of the main bands at about 1085 cm^{-1}. The infrared spectra of the acid-based geopolymer cements show the adsorption bands at 1634 and 3390 cm^{-1} which are assigned to the bending and stretching vibration modes of O–H of water molecules and Si–OH or P–OH bonds, respectively. Those at 464 and 528 cm^{-1} are assigned to the bending vibrations of siloxane (Si–O–Si) and alumino-phospho (Al–O–P) bonds, respectively [36, 37]. The presence of alumino-phospho bonds could be related to the formation of the amorphous aluminium phosphate hydrate ($AlPO_4 \cdot 2H_2O$) in the structure of the acid-based geopolymers [14, 36] and augelite in the specimens obtained when
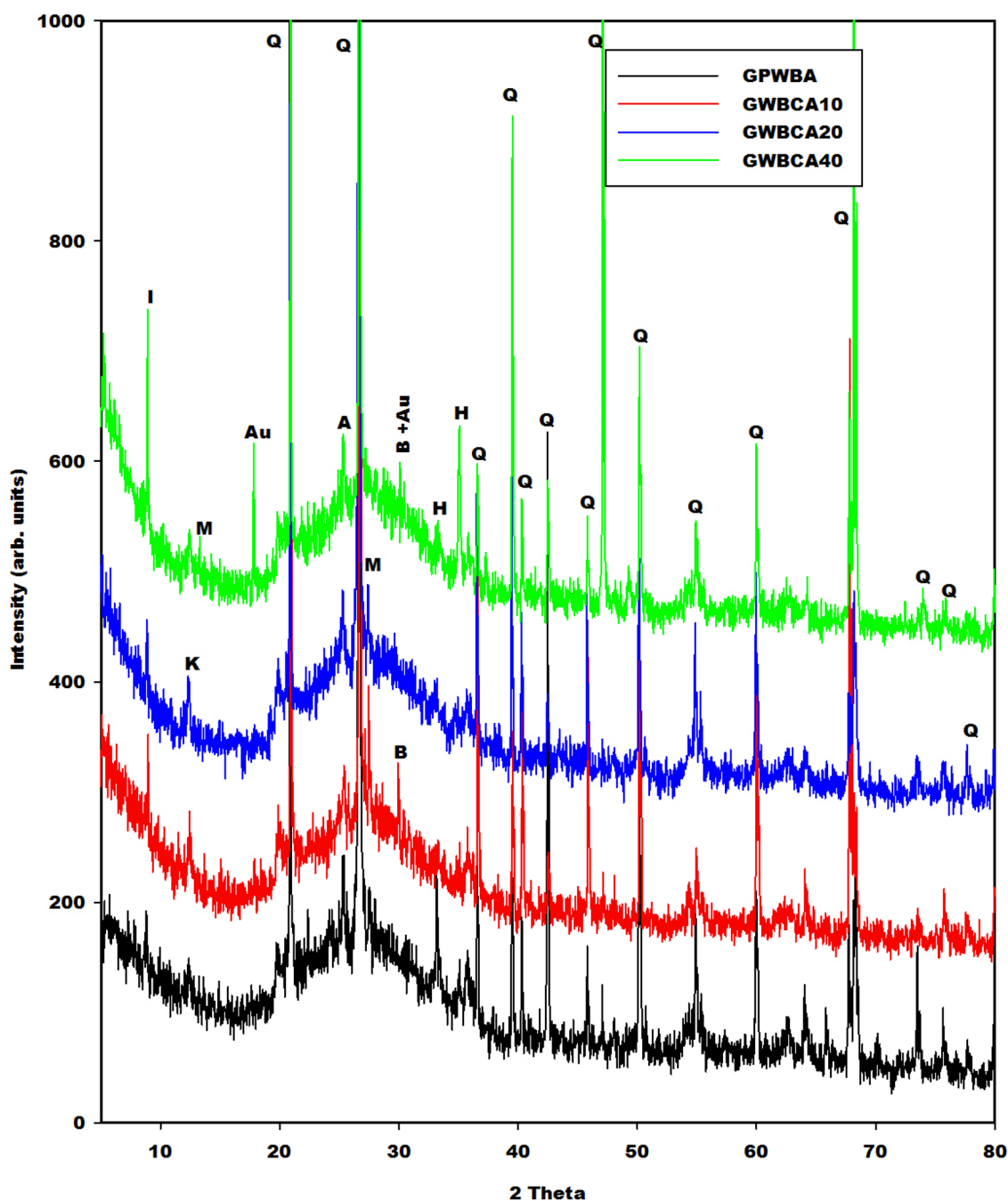
Fig. 9 (continued)

semi-crystalline calcium aluminate hydrate was added to the waste fired brick. The bands at 694 and 777 cm^{-1} are ascribed to the stretching vibrations of siloxane (Si–O–Si) bonds of quartz [29]. The absorption bands at about 796 and 908 cm^{-1} are attributed to the stretching vibrations of phospho-siloxane (Si–O–P) and P–OH bonds, respectively [22, 36]. The band of the phospho-siloxane is superimposed with the one of quartz which appears at 799 cm^{-1}

on the infrared spectrum of waste fired brick (Fig. 6). The absorption band that appears at 1085 cm^{-1} on the spectra of GPWBA, GWBEg10, GWBEg20, GWBEg40, GWBCA10, GWBCA20, GWBCA40 and those that appear at 1087, 1088 and 1090 cm^{-1} on the spectra of GWBCS10, GWBCS20 and GWBCS40, respectively are recorded to the formation of the poly(phospho-siloxane) chains. By comparison to the spectrum of waste fired brick (Fig. 6), these bands shift towards high frequencies
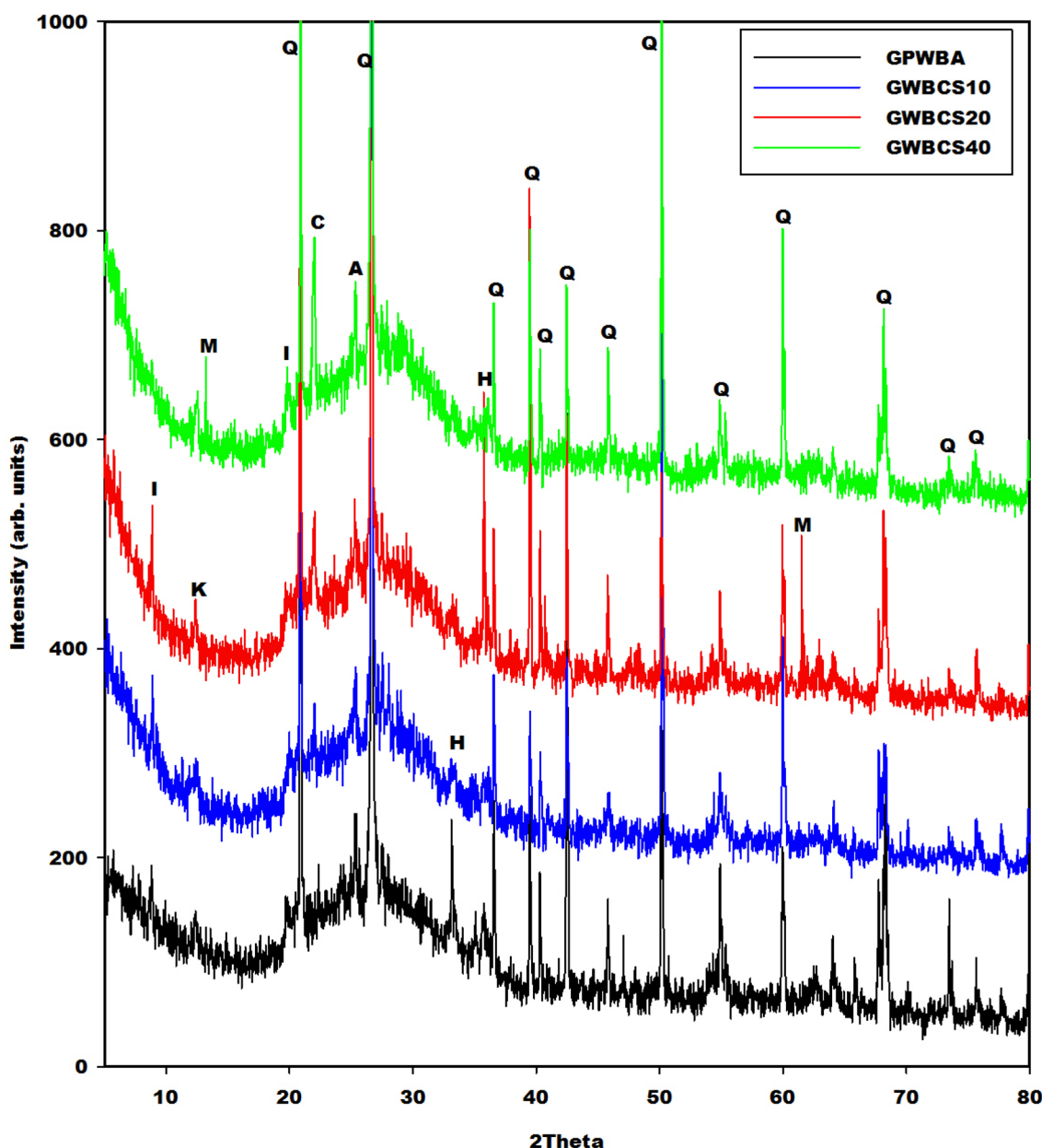
Fig. 9 (continued)

in poly(phospho-siloxane) binder. The shift is approximately 21 cm^{-1} for the GPWBA, GWBEg10, GWBEg20, GWBEg40, GWBCA10, GWBCA20, GWBCA20 and 23, 24 and 26 cm^{-1} for GWBCS10, GWBCS20 and GWBCS40, respectively. This demonstrates a change of microstructure takes place during the depolymerisation and polycondensation process resulting in the formation of the new products with a different microstructure of the one of waste fired brick. This is in agreement with the X-ray patterns which show the displacement of the broad band that appears in the waste fired brick at between 15 and 32°(2θ) (Fig. 3) towards higher °2θ [18–38°(2θ)] on

the diffractograms of the acid-based geopolymer cements (Fig. 9).

3.2.3 Compressive Strengths

Figure 11 presents the compressive strength values of the acid-based geopolymer cements after adding 0, 10, 20, 40 and 50 g of calcined eggshell, semi-crystalline calcium aluminate hydrate and semi-crystalline calcium silicate hydrate to 100 g of waste fired brick. This figure shows that the compressive strength values of the specimens GPWBA, GWBEg10, GWBEg20, GWBEg40 and GWBEg50 are
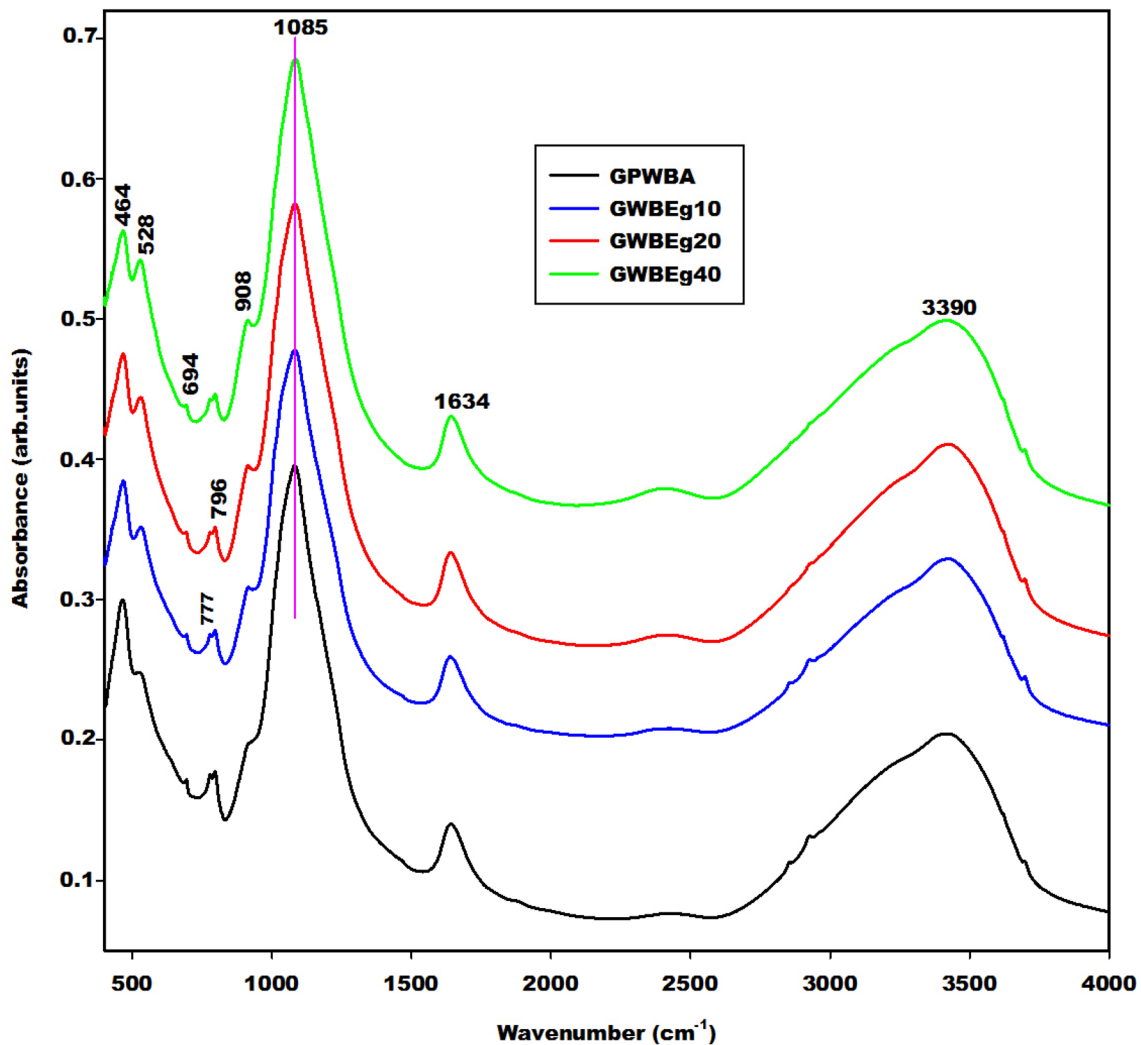
Fig. 10 Infrared spectrums of the acid-based geopolymers

56.43, 30.15, 22.85, 21.16 and 13.47 MPa, respectively. The ones of GWBCA10, GWBCA20, GWBCA40 and GWBCA50 are 32.61, 31.58, 17.83 and 16.33 MPa, respectively. Those of GWBCS10, GWBCS20, GWBCS40 and GWBCS50 are 44.02, 42.71, 40.19 and 18.59 MPa, respectively. It can be seen that the compressive strengths of the acid-based geopolymer cements decrease with increasing the addition of any calcium sources used in this investigation. The reduction of the compressive strengths when calcium sources are added to the waste fired brick could be related to the fact that one part of phosphoric acid solution reacts with calcium sources. Others react with alumina owing to the dealumination of waste fired brick. The formation of calcium phosphates such as monetite and brushite when Eggshell_900, monetite and augelite when semi-crystalline calcium aluminate hydrate, monetite and silanol groups when calcium silicate are added to the waste fired brick (Fig. 9) contributes to decreasing the amount of the

poly(phospho-siloxo) binder in the structure of the acid-based geopolymer cements. The formation of the calcium phosphate compounds with sponge-like structure [38] or plate-like particles [39, 40] in the structure of the acid-based geopolymers cannot bind to the poly(phospho-siloxo) chains and not able to act as micro-aggregate like CSH. It was found that the addition of the calcium sources in the structure of the starting material during the synthesis of the acid-based geopolymers affects negatively its compressive strength. By contrary, when an aluminosilicate source was substituted by calcium source for producing geopolymer cement using an alkaline solution, the compressive strength increases up to 20 wt% of the addition of any calcium silicate [11, 12, 41] owing to the formation of calcium silicate hydrate phase which is responsible for the compressive strength development. This could be assigned to the plate-like morphology of CSH which tends to stack into agglomerates [42]. It appears that the compressive strengths of the acid-based
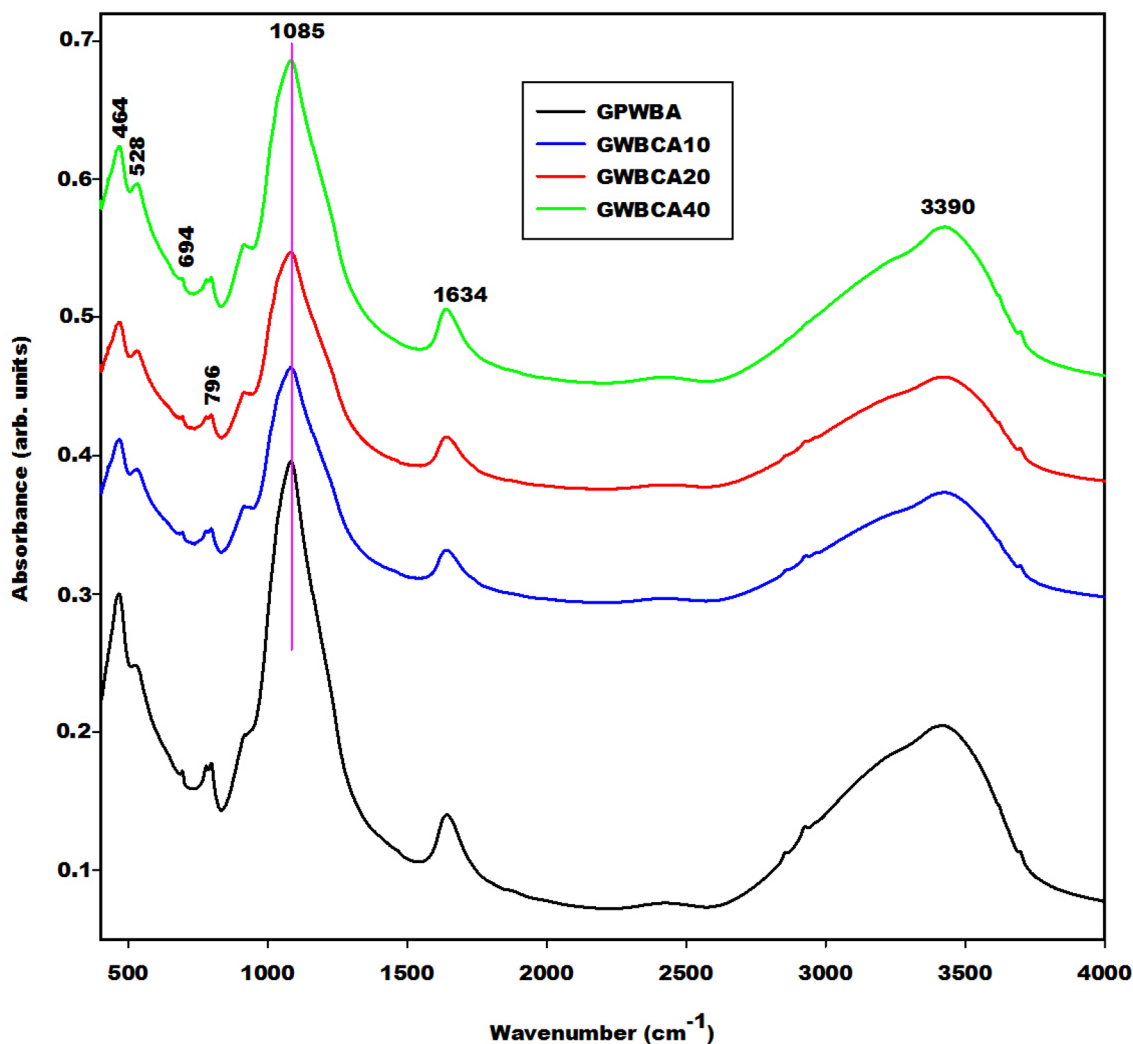
Fig. 10 (continued)

geopolymers after adding 10, 20 and 40 g of calcium silicate hydrate to 100 g of waste fired brick are nearly the same values (between 40 and 44 MPa). This could be ascribed to the amorphous silica contains in the semi-crystalline calcium silicate hydrate which produces the additional silanol groups during the depolymerisation of the waste fired brick, according to Eq. (5). These silanol groups condensed with silicon-phosphate [Si–O–PO(OH)$_2$] during the polycondensation process forming more siloxane chains in the network of poly(phospho-siloxane) and therefore maintain its strength between 40 and 44 MPa. The drastically drop of the compressive strength of the acid-based geopolymer cement when 50 g of the semi-crystalline calcium silicate hydrate was added to 100 g of waste fired brick could be assigned to the excess of monetite or silanol groups in the network and probably low silicon-phosphate. The drastically reduction of the compressive strengths when 20 g of the semi-crystalline calcium aluminate hydrate was added to 100 g of the waste fired brick (from 31.58 to 16.33 MPa) is assigned to the formation of the excess augelite which reduces the poly(phospho-siloxo) chains. This impedes the polycondensation process and therefore decrease strongly the compressive strength.

3.2.4 Micrography Images

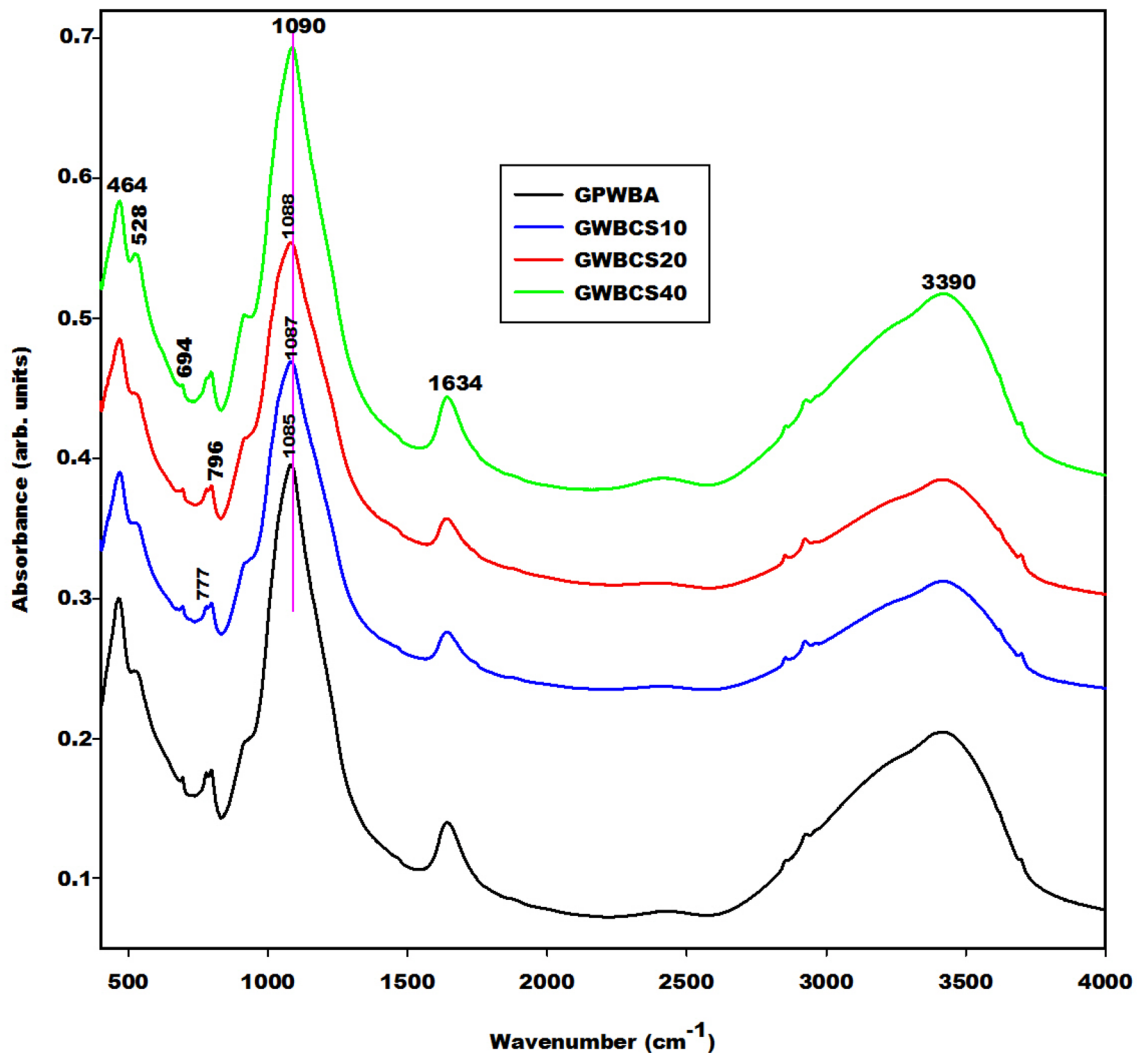Figure 12 shows the micrography images of the selected acid-based geopolymer cements at ×100 and ×1000

Fig. 10 (continued)

magnifications. This figure indicates that the micrography images of the phosphate-based geopolymer cements without the addition of calcium source denoted GPWBA are compact, homogeneous and denser microstructure with a smooth surface. The denser matrix of this specimen could be related to the well-connected of the poly(phospho-siloxo) particles. This is responsible for its high compressive strength (56.43 MPa) indicating the higher degree of polycondensation compared to those obtained by the addition of calcium sources to waste fired brick. The surface of the acid-based geopolymer cements obtained by the addition of calcium sources (Eggshell_900, CA and CS) to the waste fired brick is roughed. This could be related to the formation of calcium phosphates such as monetite and brushite which do not form a homogeneous phase with the poly(phospho-siloxo) networks, resulting in decreased the compressive strengths of the acid-based geopolymers. This implies that calcium phosphates are not connected to the poly(phospho-siloxane) chains and therefore contribute to weakening the structure of the final products. The microcracks observed in the micrography images of the control acid-based geopolymer (GPWBA) could be attributed to the formation of the hard block of poly(phospho-siloxo) which withstood during their contact with the driven testing machine. This withstand
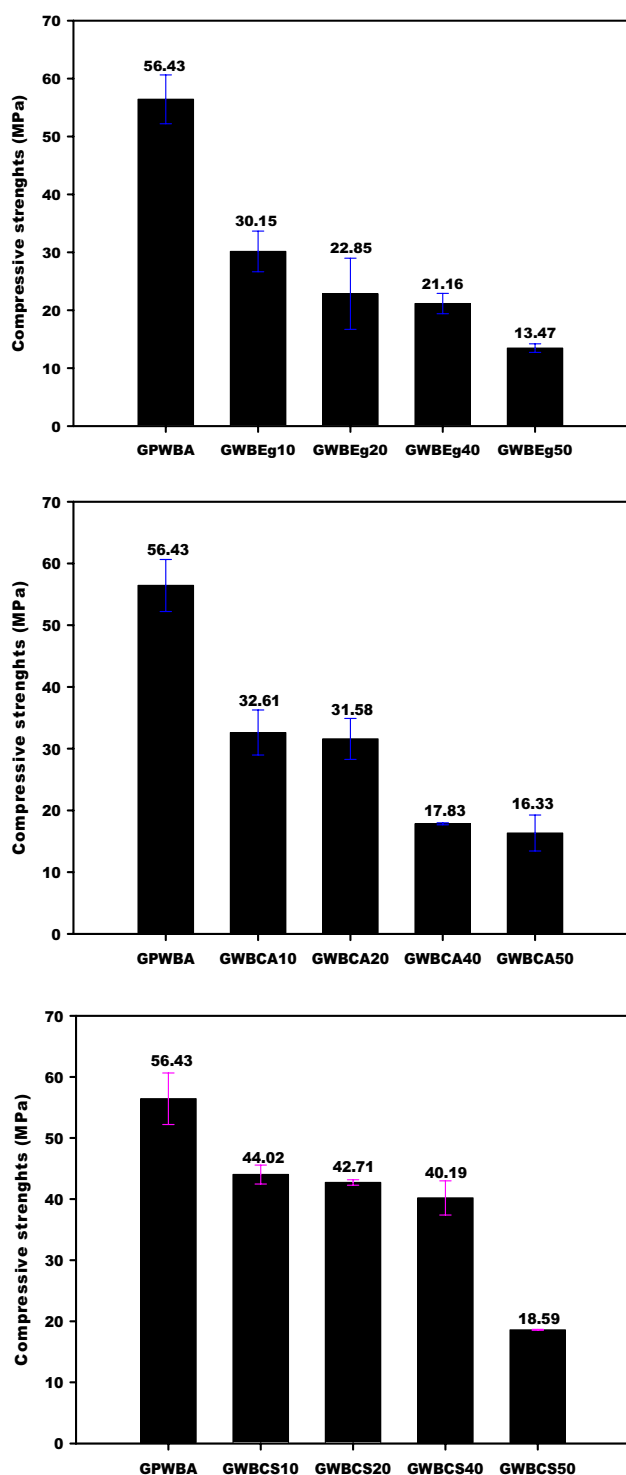
Fig. 11 Compressive strengths of the acid-based geopolymers

is related to the more condensed geopolymer structure and justify the higher strength of control acid-based geopolymer (56.43 MPa). Whereas, these cracks are more pronounced in the micrography images of the specimens containing calcium sources (Eggshell_900, CA and CS) owing to the formation of different calcium phosphates formed in the network which contribute to reduce of the poly(phosphosiloxo) chains.

4 Conclusion

Semi-crystalline calcium silicate hydrate and semi-crystalline calcium aluminate hydrate with the molar ratios SiO_2/CaO and Al_2O_3/CaO, respectively equal to 1.0 were prepared using calcined bauxite as an alumina source, rice hush ash as a silica source and calcined eggshell as a calcium source. Calcined eggshell, the prepared semi-crystalline calcium silicate hydrate and calcium aluminate hydrate were added to the waste fired brick (aluminosilicate source) in order to investigate the coexistence of the poly(phosphosiloxo) networks and calcium phosphates formed in the structure of the acid-based geopolymers obtained at room temperature on their compressive strengths. It appears that the X-ray patterns of the acid-based geopolymers using calcined eggshell as calcium source indicate the reflection peaks of monetite and brushite, those using semi-crystalline calcium aluminate hydrate show the reflection peaks of monetite and augelite. Whereas those from the semi-crystalline calcium silicate hydrate present the peaks of monetite. The additional silanol groups from the depolymerisation of the semi-crystalline calcium silicate hydrate during the polycondensation process condenses with the silicon-phosphate forming a three-dimensional poly(phospho-siloxo) networks. The compressive strength of the acid-based geopolymers from waste fired brick without added calcium sources is 56.43 MPa. Those of the specimens after added calcined eggshell, semi-crystalline calcium aluminate and calcium silicate hydrates are ranging from 13.47 to 30.15 MPa, 16.33 to 32.62 MPa and 18.59 to 44.02 MPa, respectively. It can be seen that the compressive strengths decrease when calcium sources should be added but remain higher (between 40.19 and 44.02 MPa) when 10, 20 and 40 g of semi-crystalline calcium silicate hydrate was added to the waste fired brick. Semi-crystalline calcium silicate hydrate provides acid-based geopolymers with compressive strength comparable to the Ordinary Portland cement CEM II 42.5 MPa. It can
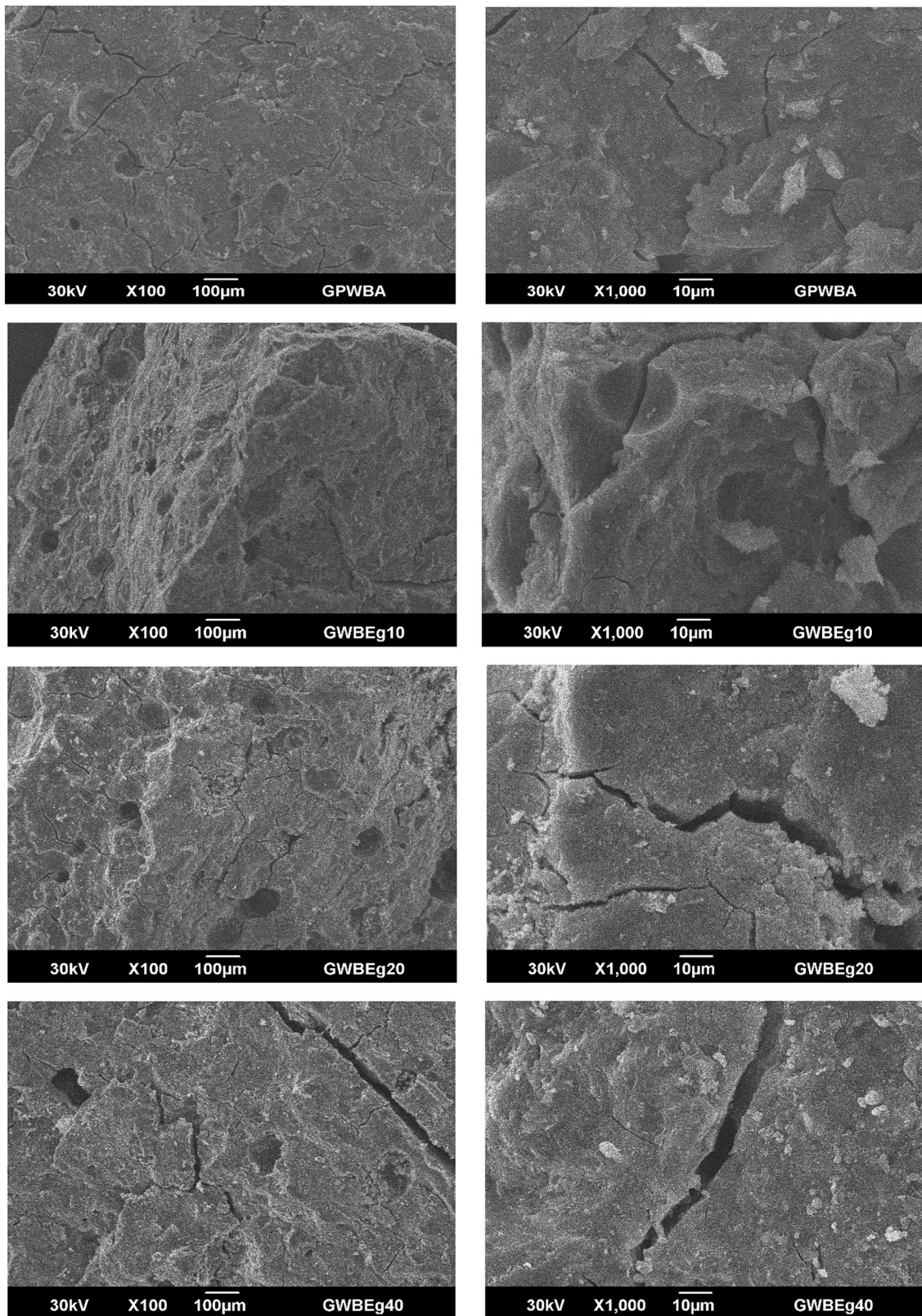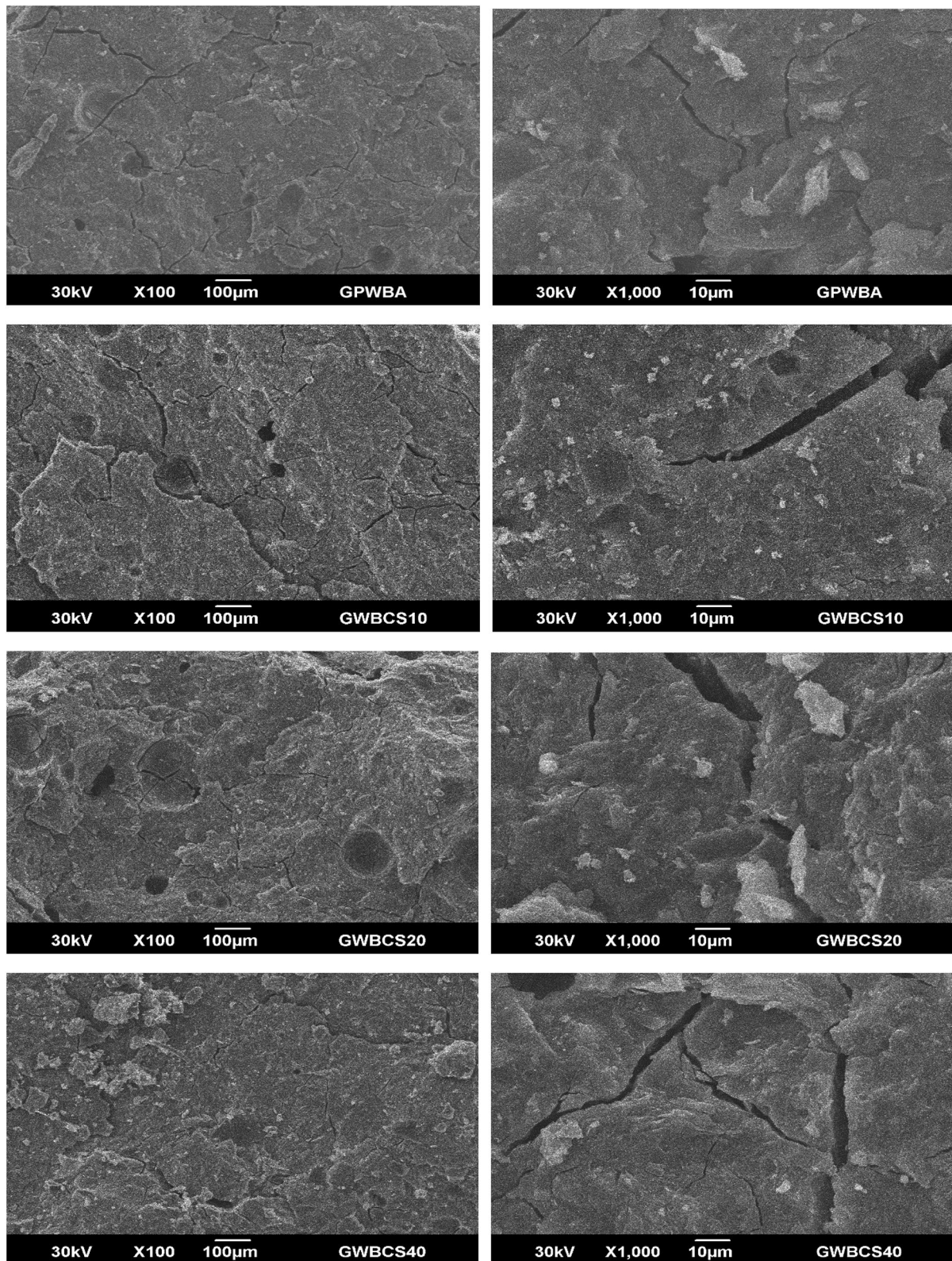
Micrography images of acid-based geopolymer cements obtained by mixing 0, 10, 20 and 40 g of Eggshell_900 to 100 g of waste fired brick.

Fig. 12 Micrography images of the selected acid-based geopolymer cements
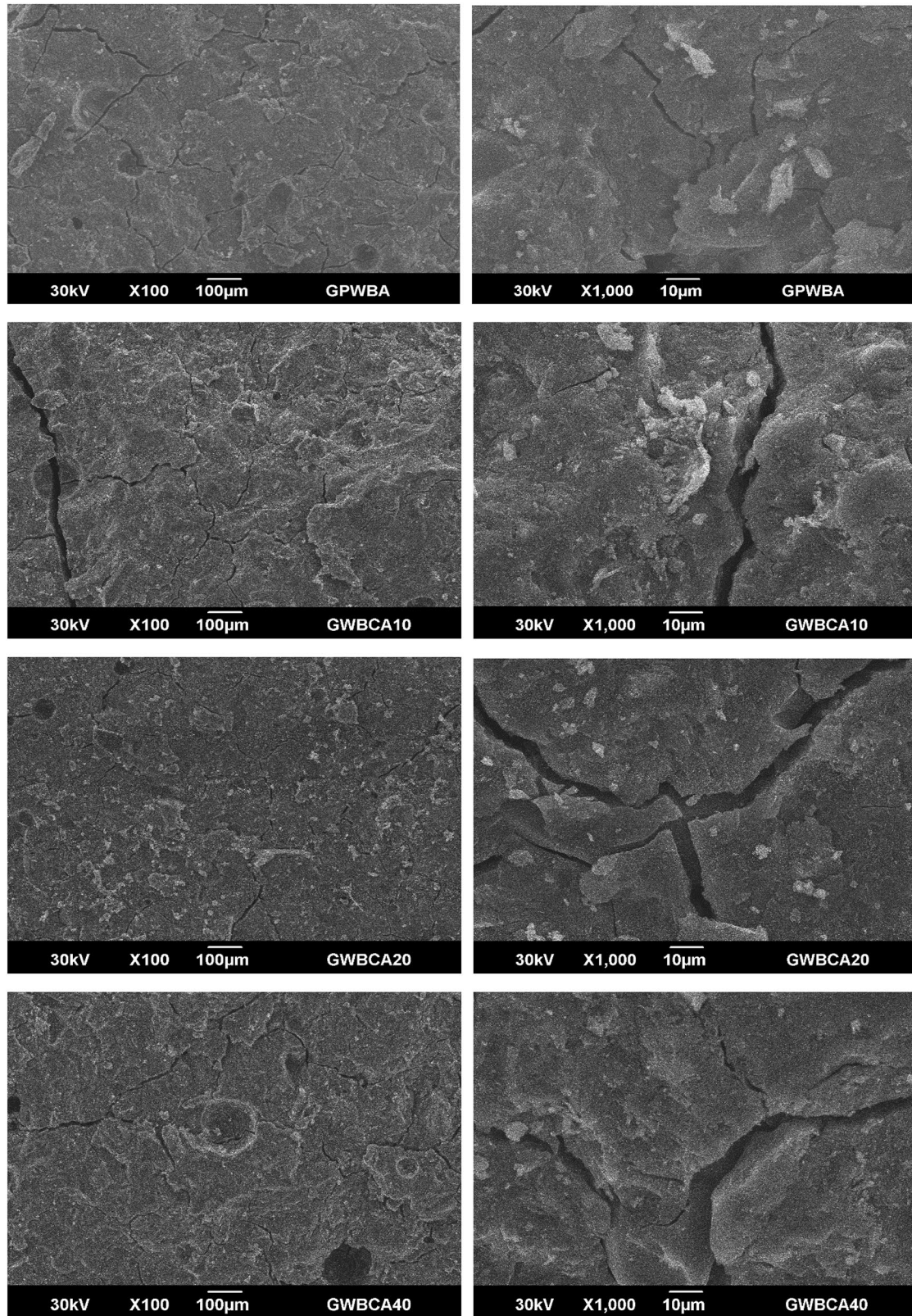
Micrography images of acid-based geopolymer cements obtained by mixing 0, 10, 20 and 40 g of CA to 100 g of waste fired brick.

Fig. 12 (continued)

Micrography images of acid-based geopolymer cements obtained by mixing 0, 10, 20 and 40 g of CS to 100 g of waste fired brick.

Fig. 12 (continued)

be concluded that the formation of the calcium phosphates in the structure of the acid-based geopolymers could reduce the amount of the binder (poly(phospho-siloxo chains) and therefore reduces the compressive strengths. Based on the results obtained in this work, the aluminosilicate sources used for the synthesis of the acid-based geopolymers must not have high calcium oxide content.

Declarations

Conflict of interest No potential conflict of interest was reported by the authors.

References

1. C.Y. Heah, H. Kamarudin, A.M.M. Al Bakri, M. Luqman, I. Khairul Nizar, Y.M. Liew, Potential application of kaolin without calcined as greener concrete: a review. Aust. J. Basic Appl. Sci. **5**, 1026–1035 (2011)
2. E. Kamseu, C. Leonelli, D.S. Perera, U.F.C. Melo, P.N. Lemougna, Investigation of volcanic ash-based geopolymers as potential building materials. Int. Ceram. **58**, 136–140 (2009)
3. D. Bondar, C.J. Lynsdale, N.B. Milestone, N. Hassani, A.A. Ramezanianpour, Effect of heat treatment on reactivity-strength of alkali-activated natural pozzolans. Constr. Build. Mater. **25**, 4065–4071 (2011)
4. D. Bondar, C.J. Lynsdale, N.B. Milestone, N. Hassani, A.A. Ramezanianpour, Effect of adding mineral additives to alkali-activated natural pozzolan paste. Constr. Build. Mater. **25**, 2906–2910 (2011)
5. P.N. Lemougna, K.J.D. Mackenzie, U.F.C. Melo, Synthesis and thermal properties of inorganic polymers (geopolymers) for structure and refractory applications from volcanic ash. Ceram. Int. **37**, 3011–3018 (2011)
6. H.K. Tchakouté, A. Elimbi, E. Yanne, C.N. Djangang, Utilization of volcanic ashes for the production of geopolymers cured at ambient temperature. Cem. Concr. Comp. **38**, 75–81 (2013)
7. W.K.W. Lee, J.S.J. van Deventer, Structural reorganisation of class F fly ash in alkaline solutions. Colloids Surf. A **211**, 49–66 (2002)
8. X. Guo, H. Shi, W.A. Dick, Compressive strength and microstructural characteristics of class C fly ash geopolymer. Cem. Concr. Comp. **32**, 142–147 (2010)
9. T.W. Cheng, J.P. Chiu, Fire resistant geopolymer produced by granulated blast furnace slag. Miner. Eng. **16**, 205–210 (2003)
10. A. Elimbi, H.K. Tchakoute, D. Njopwouo, Effects of calcination temperature of kaolinite clays on the properties of geopolymers cements. Constr. Build. Mater. **25**, 2805–2812 (2011)
11. C.K. Yip, G.C. Lukey, J.L. Provis, J.S.J. van Deventer, Effect of calcium silicate sources on geopolymerization. Cem. Concr. Res. **38**, 554–564 (2008)
12. C.K. Yip, G.C. Lukey, J.S.J. van Deventer, The coexistence of geopolymeric gel and calcium silicate hydrate at the early stage of alkaline activation. Cem. Concr. Res. **35**, 1688–1697 (2005)
13. D.E.T. Mabah, H.K. Tchakouté, C.H. Rüscher, E. Kamseu, A. Elimbi, C. Leonelli, Design of low-cost semi-crystalline calcium

14. silicate from biomass for the improvement of the mechanical and microstructural properties of metakaolin-based geopolymer cements. Mater. Chem. Phys. **223**, 98–108 (2019)
14. H.K. Tchakouté, D.E.T. Mabah, C.H. Rüscher, E. Kamseu, F. Andreola, M.C. Bignozzi, C. Leonelli, Preparation of low-cost nano and microcomposites from chicken eggshell, nano-silica and rice husk ash and their utilisations as additives for producing geopolymer cements. J. Asian Ceram. Soc. **8**, 149–161 (2020)
15. K.J.D. MacKenzie, M.E. Smith, A. Wong, A multinuclear MAS NMR study of calcium-containing aluminosilicate inorganic polymers. J. Mater. Chem. **17**, 5090–5096 (2007)
16. F.M. Tchuenté, H.K. Tchakouté, C. Banenzoué, C.H. Rüscher, E. Kamseu, F. Andreola, C. Leonelli, Microstructural and mechanical properties of (Ca, Na)-poly(sialate-siloxo) from metakaolin as aluminosilicate and calcium silicate from precipitated silica and calcined chicken eggshell. Constr. Build. Mater. **201**, 662–675 (2019)
17. H.K. Tchakouté, D. Fotio, C.H. Rüscher, E. Kamseu, J.N.Y. Djobo, M.C. Bignozzi, C. Leonelli, The effects of synthesized calcium phosphate compounds on the mechanical and microstructural properties of metakaolin-based geopolymer cements. Constr. Build. Mater. **163**, 776–792 (2018)
18. M.L. Gualtieri, M. Romagnoli, A.F. Gualtieri, Preparation of phosphoric acid-based geopolymer foams using limestone as pore forming agent-thermal properties by in situ XRPD and Rietveld refinements. J. Eur. Ceram. Soc. **35**, 3167–3178 (2015)
19. N. Boutaleb, F. Chouli, A. Benyoucef, F.Z. Zeggai, K. Bachari, A comparative study on surfactant cetyltrimethylammoniumbromide modified clay-based poly(p-anisidine) nanocomposites: synthesis, characterization, optical and electrochemical properties. Polym. Compos. (2021). https://doi.org/10.1002/pc.25941
20. D. Cao, D. Su, B. Lu, Y. Yang, Synthesis and structure characterization of geopolymeric material based on metakaolinite and phosphoric acid. J. Chin. Ceram. Soc. **33**, 1385–1389 (2005)
21. D.S. Perera, J.V. Hanna, J. Davis, The relative strength of phosphoric acid-reacted and alkali-reacted metakaolin materials. J. Mater. Sci. **43**, 6562–6566 (2008)
22. H. Celerier, J. Jouin, V. Mathivet, N. Tessier-Doyen, S. Rossignol, Composition and properties of phosphoric acid-based geopolymers. J. Non-Cryst. Solids **493**, 94–98 (2018)
23. M.L. Gualtieri, M. Romagnoli, S. Pollastri, A.F. Gualtieri, Inorganic polymers from laterite using activation with phosphoric acid and alkaline sodium silicate solution: mechanical and microstructural properties. Cem. Concr. Res. **67**, 259–270 (2015)
24. C.N. Bewa, H.K. Tchakouté, C.H. Rüscher, E. Kamseu, C. Leonelli, Influence of the curing temperature on the properties of poly(phospho-ferro-siloxo) networks from laterite. SN Appl. Sci. **1**, 1–12 (2019)
25. J. Davidovits, *Geopolymer Chemistry and Applications*, 3rd edn. (Institute Geopolymer, Saint-Quentin, 2011), p. 612
26. C.N. Bewa, H.K. Tchakouté, C. Banenzoué, L. Cakanou, T.T. Mbakop, E. Kamseu, C.H. Rüscher, Acid-based geopolymers using waste fired brick and different metakaolins as raw materials. Appl. Clay Sci. **198**, 105813 (2020)
27. A.B. Tchamba, R. Yongue, U.F.C. Melo, E. Kamseu, D. Njoya, D. Njopwouo, Caractérisation de la bauxite de Haléo-Danielle (Minim-Martap, Cameroun) en vue de son utilisation industrielle dans les matériaux à haute teneur en alumine. Silic. Ind. **73**, 77–83 (2008)
28. D. Prasetyoko, Z. Ramli, S. Endud, H. Hamdan, B. Sulikowski, Conversion of rice husk ash to zeolite beta. Waste Manag. **26**, 1173–1179 (2006)
29. H.K. Tchakouté, C.H. Rüscher, J.N.Y. Djobo, B.B.D. Kenne, D. Njopwouo, Influence of gibbsite and quartz in kaolin on the

properties of metakaolin-based geopolymer cements. Appl. Clay Sci. **107**, 188–194 (2015)

30. R.L. Frost, J.T. Kloprogge, S.C. Russell, J.L. Szetu, Vibrational spectroscopy and dehydroxylation of aluminum (oxo)hydroxides: gibbsite. Appl. Spectrosc. **53**, 423–434 (1999)

31. R.L. Frost, J.T. Kloprogge, S.C. Russell, J.L. Szetu, Dehydroxylation and the vibrational spectroscopy of aluminum (oxo)hydroxides using infrared emission spectroscopy. Part III: diaspore. Appl. Spectrosc. **53**, 829–835 (1999)

32. A. Boumaza, L. Favaro, J. Lédion, G. Sattonnay, J.B. Brubach, P. Berthet, A.M. Hunt, P. Roy, R. Tétot, Transition alumina phases induced by heat treatment of boehmite: an X-ray diffraction and infrared spectroscopy study. J. Solid State Chem. **182**, 1171–1176 (2009)

33. X. Pan, D. Zhang, Y. Wu, H. Yu, Synthesis and characterization of calcium aluminate compound from gehlenite by high-temperature solid state reaction. Ceram. Int. **44**, 13544–13550 (2018)

34. Z. Zidi, M. Ltifi, Z. Ben Ayadi, L. ElMir, Synthesis of nano-alumina and their effect on structure, mechanical and thermal properties of geopolymer. J. Asian Ceram. Soc. **7**, 524–535 (2019)

35. K. Baltakys, R. Jauberthie, R. Siauciunas, R. Kaminskas, Influence of modification of SiO_2 on the formation of calcium silicate hydrate. Mater. Sci. Poland **25**, 663–670 (2007)

36. C.N. Bewa, H.K. Tchakouté, D. Fotio, C.H. Rüscher, E. Kamseu, C. Leonelli, Water resistance and thermal behaviour of metakaolin-phosphate-based geopolymer cements. J. Asian Ceram. Soc. **6**, 271–283 (2018)

37. B. Zhang, H. Guo, P. Yuan, L. Deng, X. Zhong, Y. Li, Q. Wang, D. Liu, Novel acid-based geopolymer synthesized from nanosized tubular halloysite: the role of precalcination temperature and phosphoric acid concentration. Cem. Concr. Comp. **110**, 103601 (2020)

38. J. Wang, H. Zhao, S. Zhou, X. Lu, B. Feng, C. Duan, J. Weng, One-step in situ synthesis and characterization of sponge-like porous calcium phosphate scaffolds using a sol-gel and gel casting hybrid process. J. Biomedical Mater. Res. Part A **90A**, 401–410 (2009)

39. R. Štulajterová, L. Medvecky, Effect of calcium ions on transformation brushite to hydroxyapatite in aqueous solutions. Colloids Surf. A **316**, 104–109 (2008)

40. M.M. Mirkovic, T.D.L. Pašti, A.M. Došen, M.Z. Cebela, A.A. Rosic, B.Z. Matovic, B.M. Babic, Adsorption of malathion on mesoporous monetite obtained by mechanochemical treatment of brushite. RSC Adv. **6**, 12219–12225 (2016)

41. C.K. Yip, The role of calcium in geopolymerization, University of Melbourne, Australia, PhD Thesis (2004)

42. A. Moshiri, D. Stefaniuk, S.K. Smith, A. Morshedifard, D.F. Rodrigues, M.J.A. Qomi, K.J. Krakowiak, Structure and morphology of calcium-silicate-hydrates cross-linked with dipodal organosilanes. Cem. Concr. Res. **133**, 106076 (2020)